

The Formation and Early Evolution of Low-mass Stars and Brown Dwarfs

KEVIN L. LUHMAN^{1,2}

¹ *Department of Astronomy and Astrophysics, The Pennsylvania State University, University Park, PA 16802, USA; kluhman@astro.psu.edu*

² *Center for Exoplanets and Habitable Worlds, The Pennsylvania State University, University Park, PA 16802, USA*

Key Words star formation, pre-main-sequence evolution, circumstellar disks, protostars, spectral classification, stellar multiplicity, star-forming regions, young associations, open clusters, initial mass function

Abstract

The discovery of large numbers of young low-mass stars and brown dwarfs over the last decade has made it possible to investigate star formation and early evolution in a previously unexplored mass regime. In this review, we begin by describing surveys for low-mass members of nearby associations, open clusters, star-forming regions and the methods used to characterize their stellar properties. We then use observations of these populations to test theories of star formation and evolution at low masses. For comparison to the formation models, we consider the initial mass function, stellar multiplicity, circumstellar disks, protostellar characteristics, and kinematic and spatial distributions at birth for low-mass stars and brown dwarfs. To test the evolutionary models, we focus on measurements of dynamical masses and empirical Hertzsprung-Russell diagrams for young brown dwarfs and planetary companions.

Posted with permission from the Annual Review of Astronomy and Astrophysics, Volume 50 ©2012 by Annual Reviews, <http://www.annualreviews.org>.

CONTENTS

INTRODUCTION	2
SURVEYS FOR YOUNG LOW-MASS STARS AND BROWN DWARFS	3
<i>Search Strategies</i>	3
<i>Young Associations and Moving Groups</i>	4
<i>Young Open Clusters</i>	6
<i>Star-Forming Regions</i>	7
<i>Characterization of Stellar Properties</i>	10
FORMATION AT LOW MASSES	14
<i>Theory</i>	14
<i>Initial Mass Function</i>	15
<i>Multiplicity</i>	17
<i>Circumstellar Disks</i>	19
<i>Protostars</i>	21
<i>Kinematics and Positions at Birth</i>	22

EARLY STELLAR EVOLUTION AT LOW MASSES	23
<i>Theory</i>	23
<i>Rotation</i>	24
<i>Dynamical Masses</i>	25
<i>Hertzsprung-Russell Diagram</i>	27
<i>Accuracy of IMF Measurements in Young Clusters</i>	30
Concluding Remarks	30
Sidebar	42
<i>The Discovery of Brown Dwarfs</i>	42

1 INTRODUCTION

Molecular clouds give birth to stars across a wide range of masses. The most massive stars are born on the main sequence while low-mass stars must contract for tens to hundreds of millions of years before becoming hot enough for sustained hydrogen fusion. A great deal of observational and theoretical effort has been invested in understanding star formation and pre-main-sequence evolution and their dependence on stellar mass. Over the last decade, it has become possible to extend these studies to the least massive stars and brown dwarfs as surveys have uncovered them in large numbers and at a variety of ages. In this way, star formation and early evolution can be investigated across more than four orders of magnitude in stellar mass, providing more stringent tests of the theories for these processes.

In this review, we summarize the theoretical and observational work on the formation and early evolution of low-mass stars and brown dwarfs. We define a “low-mass star” as having a mass between $\sim 0.2 M_{\odot}$ and the hydrogen burning mass limit ($\sim 0.075 M_{\odot}$, Burrows et al. 1997, Chabrier & Baraffe 2000). All free-floating objects (as well as some companions) below this mass range are considered brown dwarfs. Some studies have adopted the deuterium burning limit ($\sim 0.012 M_{\odot}$, Chabrier et al. 2000a; Spiegel, Burrows & Milsom 2011) as the lower limit for the definition of a brown dwarf (Basri 2000), but this is not done here since deuterium burning has a negligible impact on stellar structure and evolution (Chabrier et al. 2007). Since we are examining the formation and early evolution of low-mass stars and brown dwarfs, we focus on objects with ages $\lesssim 100$ Myr, which is the time-scale for low-mass stars to approach the main sequence. However, we also consider the properties of older stars and brown dwarfs that can help constrain the formation and evolutionary theories, such as their multiplicity and mass function.

This article complements previous reviews concerning low-mass stars and brown dwarfs. Basri (2000) reviewed early discoveries of brown dwarfs and Kirkpatrick (2005) reviewed the spectral classification of (mostly older) L and T dwarfs, whereas we focus on the discovery and characterization of low-mass stars and brown dwarfs at young ages. Whitworth et al. (2007) and Chabrier & Baraffe (2000) reviewed theories for the formation and evolution of brown dwarfs, respectively, and Luhman et al. (2007d) and Burgasser et al. (2007) compared the predictions of the formation models to observations. We summarize the latest developments in those theories and update the previous reviews of the observational constraints on the formation of brown dwarfs.

2 SURVEYS FOR YOUNG LOW-MASS STARS AND BROWN DWARFS

2.1 Search Strategies

Studies of the formation and early evolution of low-mass stars and brown dwarfs have been enabled by surveys that discover and characterize these objects, particularly at young ages. The targets of these surveys have consisted of the nearest young associations, open clusters, and star-forming regions ($d = 50\text{--}500$ pc, $\tau = 1\text{--}100$ Myr). Young brown dwarfs are brightest at near-infrared (IR) wavelengths ($1\text{--}2$ μm , *YJHK*), but because of their relatively warm temperatures, they often can be detected in red optical bands as well ($0.6\text{--}1$ μm , *RIZ*). In fact, an optical filter is quite helpful for identifying red, late-type objects when combined with data at longer wavelengths. As a result, surveys for young brown dwarfs often have employed both optical and near-IR images. These data have been collected through both dedicated imaging and wide-field surveys. Examples of the latter include the Two Micron All-Sky Survey (2MASS, Skrutskie et al. 2006), the Deep Near-Infrared Survey of the Southern Sky (DENIS, Epchtein et al. 1999) the Sloan Digital Sky Survey (SDSS, York et al. 2000), and the United Kingdom Infrared Telescope Infrared Deep Sky Survey (UKIDSS, Lawrence et al. 2007).

To identify candidate low-mass stars and brown dwarfs, images are searched for objects that have colors/magnitudes or proper motions that are indicative of membership in the target cluster or association. If the images are deep enough and an appropriate combination of filters is present, it is actually easier to identify cool dwarfs than many other classes of astronomical sources because of the distinctive nature of their spectral energy distributions (SEDs), which results from strong molecular absorption bands. However, a few words of caution are warranted regarding photometric searches. First, some studies have designed their photometric criteria for the selection of candidates based on theoretical magnitudes and colors that are predicted for the age of the target cluster or association. However, model colors are often too inaccurate for this purpose. Instead, it is better to use the photometry of known young low-mass objects, either in the target population or in others with a similar age, to guide the identification of candidates. If this is not possible, then the theoretical predictions for temperature and luminosity should be converted to magnitudes and colors using empirical relations between spectral types, temperatures, colors, and bolometric corrections. These relations are incomplete for young objects, but it is likely better to use the relations for dwarfs rather than rely on synthetic magnitudes. In addition to applying properly designed color and magnitude criteria, it is important to carefully account for photometric errors during the selection of candidates. For instance, near the detection limit of a given set of images, one can find sources that appear to satisfy almost any color criteria because of the large errors. A similar problem can arise when candidate low-mass members of clusters are identified through poorly constrained proper motions.

In general, it is necessary to obtain spectra of young low-mass candidates selected from photometry or proper motions to confirm their membership via measurements of radial velocities or (more commonly) signatures of youth. Spectra are also important for providing spectral types, which constrain the temperature and mass of a candidate. Low-resolution spectra are normally pre-

ferred for the initial followup of candidates since they are adequate for measuring the broad molecular absorption bands of late-type objects while also providing the highest signal-to-noise ratios. For instance, SpeX at the NASA Infrared Telescope Facility (Rayner et al. 2003) offers an ideal configuration of this kind, producing spectra from 0.8–2.5 μm with a resolution of ~ 100 . It is likely that SpeX has observed more brown dwarfs, both young and old, than any other spectrograph. Adam Burgasser maintains a compilation of a large number of these spectra of brown dwarfs in the SpeX Prism Spectral Libraries at <http://www.browndwarfs.org/spexprism>. Searches for brown dwarfs and various other kinds of rare sources (e.g., high redshift quasars, gamma ray bursts) would benefit greatly if a comparable observing mode was available on more telescopes. Additional details regarding the spectroscopic confirmation of young low-mass stars and brown dwarfs are discussed in Section 2.5.

2.2 Young Associations and Moving Groups

The nearest samples of young stars to the Sun ($d < 100$ pc) are found in small moving groups and associations (Zuckerman et al. 2011, Zuckerman & Song 2004). These stars are no longer associated with molecular clouds, and hence have ages of $\gtrsim 5$ Myr. Given their proximity and youth, they represent the best available targets for surveys to detect and resolve substellar companions and circumstellar disks. In addition, since their spectra are relatively unreddened ($A_V < 1$), members of the nearest associations are attractive candidates for spectral classification standards for young stars and brown dwarfs (Cruz, Kirkpatrick & Burgasser 2009).

If nearby groups and associations have initial mass functions (IMFs) similar to those measured in the field, open clusters, and star-forming regions, then they should contain significant populations of undiscovered low-mass stars and brown dwarfs based on the numbers of known members at higher masses. Surveys for these low-mass members have primarily employed one of two strategies: searching for candidate members of nearby associations based on data from wide-field photometric and astrometric surveys, or checking late-type dwarfs found during surveys of the field for evidence of youth or membership in any of the nearby groups. In either strategy, to firmly establish membership of a given candidate, one seeks to show that it exhibits spectroscopic indicators of youth and that it shares the same 3-D space motion as the known members, which requires measurements of parallax, proper motion, and radial velocity.

In the first of the two survey methods mentioned above, candidate low-mass members of nearby associations are initially identified based on signatures of youth and activity (X-ray, UV), late spectral type (optical, near-IR), or kinematic membership (proper motions, radial velocities). In the discovery of the first known brown dwarfs in a nearby association, Gizis (2002) used photometry from 2MASS and the Palomar Observatory Sky Survey to identify candidate late-M and L dwarfs in the direction of the TW Hya Association (TWA, $\tau \sim 10$ Myr). Through followup spectroscopy, he found that two of the candidates, 2MASSW J1207334-393254 (hereafter 2M 1207-3932) and 2MASSW J113951-3159211, exhibited spectral features that indicated low surface gravities, and hence young ages. Mohanty, Jayawardhana & Barrado y Navascués (2003) and Scholz et al. (2005) confirmed the membership of these objects via measurements of radial velocities and proper motions, respectively. Scholz et al. (2005) also used their proper motion data to uncover an additional substellar member of

TWA, SSSPM J1102-3431. These three objects have spectral types near M8.5 and are among the most widely-studied young brown dwarfs, especially 2M 1207-3932 (e.g., Sections 2.5.1, 4.4). Using photometry and proper motions from wide-field optical and near-IR surveys, Looper et al. (2007) discovered a candidate member of TWA with an even later spectral type of M9.5, DENIS J124514.1-442907. Its membership seems probable based on the evidence of youth in its optical and near-IR spectra, although radial velocity and parallax measurements are needed for a definitive assessment of membership. With the increasing availability of sensitive astrometric surveys in recent years, it has become common to use both photometry and proper motions for the selection of candidate low-mass members of young associations, which are then confirmed by radial velocity measurements (Clarke et al. 2010; Gálvez-Ortiz et al. 2010; Schlieder, Lépine & Simon 2010).

Although they are not sensitive to members at substellar masses, X-ray and UV satellites have helped to identify possible low-mass stars in nearby associations. X-ray surveys have been performed across a wide range of field sizes. For instance, deep X-ray images of small fields surrounding the B stars η Cha and ϵ Cha have uncovered compact groups of associated young low-mass stars (Feigelson, Lawson & Garmire 2003; Mamajek, Lawson & Feigelson 1999). Subsequent optical and near-IR imaging has revealed additional members of these associations at lower masses and across wider areas (Lawson et al. 2002; Luhman 2004b; Luhman & Steeghs 2004; Lyo et al. 2004; Murphy, Lawson & Bessell 2010; Song, Zuckerman & Bessell 2004). Meanwhile, Riaz, Gizis & Harvin (2006), Looper et al. (2010), and Shkolnik, Liu & Reid (2009) have used data from the *Röntgen Satellite* (ROSAT) All-Sky Survey to identify candidate young low-mass stars across much larger areas of sky. It has recently become possible to extend surveys for young stars to UV wavelengths with the availability of wide-field data from the *Galaxy Evolution Explorer* (Martin et al. 2005). Shkolnik et al. (2011) and Rodriguez et al. (2011) have found that it seems to offer better sensitivity to young low-mass stars than the all-sky data from ROSAT.

As noted above, a second approach to finding low-mass members of nearby associations is to search for them among the cool dwarfs found in surveys of the field. Within the hundreds of late-type dwarfs that they have discovered with 2MASS and other surveys, Kirkpatrick et al. (2006, 2008), Cruz et al. (2007), and Cruz, Kirkpatrick & Burgasser (2009) have identified more than two dozen late-M and L dwarfs that have gravity-sensitive spectral features indicative of youth ($\tau \lesssim 100$ Myr), and hence are promising candidates for substellar members of nearby moving groups. Similar objects have been found during other spectroscopic surveys of late-type field dwarfs (Allers et al. 2010; Nakajima, Tsuji & Yanagisawa 2004; Reiners & Basri 2010). These sources have not been definitively established as members of specific groups since complete sets of parallaxes, proper motions, and radial velocities are currently unavailable. However, Rice, Faherty & Cruz (2010) have shown that one of the young M dwarfs from Kirkpatrick et al. (2008), 2MASS 06085283-2753583, is a likely member of the β Pic moving group ($\tau \sim 12$ Myr) based on the space motion derived from its proper motion, radial velocity, and spectroscopic distance. Reiners (2009) has presented similar evidence suggesting that 2MASS J0041353-562112 (M7.5) may be a member of the Tucana/Horologium association ($\tau \sim 30$ Myr). Instead of spectroscopic signatures of youth, other studies have used proper motions (Bannister & Jameson 2007) and radial velocities (Seifahrt et al. 2010, Zapatero Osorio et al. 2007) for the initial identification of possible association members among field L and T dwarfs, but neither definitive kinematic evidence of membership nor confirmation of low gravity via

spectroscopy has been presented for these candidates to date.

2.3 Young Open Clusters

Young open clusters span the same range of ages as the nearest associations and moving groups ($\tau > 5$ Myr). The nearest examples of the former are more distant than associations like TWA ($d > 100$ pc), but they are much richer (100's–1000's of members), providing better constraints on the statistical properties of stellar populations, such as their IMF and multiplicity. In addition, open clusters are more compact on the sky, so they can be imaged in their entirety down to very faint levels.

The methods of searching for low-mass members of open clusters are similar to some of those applied to nearby associations and moving groups. The initial identification of candidate members is usually based on proper motions and/or optical color-magnitude diagrams. In early surveys, these measurements were made with photographic plates, which could detect low-mass stars in the nearest clusters. The extension of these surveys into the substellar regime became feasible in the late 1980's with the development of sensitive, large-format CCD cameras. These devices and their near-IR counterparts are now capable of imaging an entire cluster (> 10 deg²) in a reasonable amount of time. Proper motion surveys for substellar members are growing more powerful over time as the baselines from the first deep wide-field surveys steadily lengthen (Bihain et al. 2006, Casewell et al. 2007). As in young associations, candidate members of a given open cluster are confirmed by a combination of proper motions, radial velocities, and spectral signatures of youth. A subset of these diagnostics of membership is often sufficient since open clusters do not overlap with other young populations on the sky as much as nearby associations, which are much more widely distributed. This is convenient since radial velocity measurements are not feasible for the faintest brown dwarf candidates. For these objects, a spectrum showing features indicative of a cool, low gravity atmosphere is normally sufficiently convincing evidence of membership.

The most promising open clusters for detecting low-mass stars and brown dwarfs are those that are youngest and nearest ($\tau < 1$ Gyr, $d < 200$ pc), which include IC 2391 (50 Myr), α Per (90 Myr), the Pleiades (100–125 Myr), the Hyades (625 Myr), and Praesepe (~ 600 Myr). Because it offers the best combination of age, proximity, and richness, the Pleiades was the first open cluster surveyed for brown dwarfs. Proper motions measured from photographic plates were used to identify members down to $\sim 0.1 M_{\odot}$ across a large fraction of the cluster (Hambly, Hawkins & Jameson 1993). The first CCD imaging of the Pleiades covered much smaller areas (~ 0.1 deg²) but reached fainter magnitudes than the photographic data (Jameson & Skillen 1989, Stauffer et al. 1989). One of the candidates from Stauffer et al. (1989), PPl 1, was eventually confirmed as substellar through the Li test (Stauffer, Schultz & Kirkpatrick 1998), although the first brown dwarfs in the Pleiades confirmed in this manner consisted of PPl 15 and Teide 1 (Basri, Marcy & Graham 1996; Rebolo, Zapatero Osorio & Martín 1995; Rebolo et al. 1996; Stauffer, Hamilton & Probst 1994; Zapatero Osorio, Rebolo & Martín 1997). The Pleiades has been searched extensively for brown dwarfs since those initial discoveries (Moraux et al. 2003, Stauffer et al. 2007, references therein), producing a census that extends down to L spectral types and masses of $\sim 0.025 M_{\odot}$ (e.g., Martín et al. 1998). Candidate T-type members with potential masses of

$\sim 0.01 M_{\odot}$ have been found (Casewell et al. 2007, 2011), but they currently lack spectroscopic confirmation of their cool nature or youth. Surveys of the other nearby open clusters mentioned above have been quite successful as well (e.g., Barrado y Navascués, Stauffer & Jayawardhana 2004; Bouvier et al. 2008; Lodieu et al. 2005). In fact, it has been difficult for spectroscopic followup to keep pace with the large number of reported candidates, which is unfortunate since complete spectroscopic samples are valuable for addressing a number of issues regarding the formation and evolution of low-mass objects, as discussed elsewhere in this review.

2.4 Star-Forming Regions

The nearest star-forming regions ($\tau \lesssim 5$ Myr) are roughly comparable to the nearest open clusters in terms of proximity and richness. The stellar populations within the former are more difficult to identify and study because of the dust extinction from their natal molecular clouds. However, star-forming regions offer an opportunity to detect brown dwarfs when their luminosities are highest, witness the earliest stages of their formation, and examine how their properties (e.g., IMF, multiplicity) vary with star-forming conditions. The properties of embedded clusters have been reviewed by Lada & Lada (2003) and individual nearby regions have been reviewed in the *Handbook of Star Forming Regions* (B. Reipurth, ed.). The discussion in this section includes populations with ages of 5–10 Myr like Upper Sco and some of the clusters in Orion, even though they are no longer embedded within molecular clouds and thus are not experiencing ongoing star formation.

Near the same time that CCDs were first used to search for brown dwarfs in the Pleiades, early near-IR detector arrays were applied to nearby embedded clusters, often with the same objective. (CCDs also were capable of detecting the less obscured brown dwarfs in star-forming regions, but this was not yet realized.) IR surveys of Ophiuchus (Greene & Young 1992), the Trapezium Cluster (McCaughrean & Stauffer 1994), and IC 348 (Lada & Lada 1995) detected objects that are now known to be probable brown dwarfs, but they were not identified as candidates at that time. This is because near-IR broad-band filters are less sensitive to spectral type than the optical bands used in open clusters, making it more difficult to distinguish brown dwarfs from field stars. The presence of variable reddening towards the cluster members and background stars in star-forming regions further hampers reliable selection of candidates. Nevertheless, a few individual brown dwarf candidates were reported from IR imaging of embedded clusters (Comerón et al. 1993, Rieke & Rieke 1990). GY141 (ρ Oph 162349.8-242601) was one of the first candidates that was spectroscopically confirmed as a young, late-type object ($>M6$). Rieke & Rieke (1990) suggested that it was a foreground dwarf because its near-IR colors did not exhibit any reddening, but Comerón et al. (1998) identified it as a possible young brown dwarf based on the detection of mid-IR excess emission at $4.5 \mu\text{m}$ with the *Infrared Space Observatory (ISO)*, which indicated the presence of a circumstellar disk. Luhman, Liebert & Rieke (1997) used optical spectroscopy to confirm its youth and late spectral type (M8.5). Although it was a small aspect of a much larger study of the Orion Nebula Cluster (ONC), and hence received little attention at the time, Hillenbrand (1997) also presented some of the first spectral classifications of young late-type objects.

Rather than search for individual brown dwarf candidates, some of the early surveys of embedded clusters focused on statistical estimates of the substellar IMF based on IR luminosity functions. This approach was applied most extensively to the Trapezium Cluster at the center of the ONC because it is very compact and is located in front of a dense molecular cloud, reducing the contamination from background stars (Hillenbrand & Carpenter 2000; Lucas & Roche 2000; Lucas, Roche & Tamura 2005; Luhman et al. 2000; Muench et al. 2002). Other clusters have been studied in this way as well (Comerón et al. 1993, Muench et al. 2003), but because they lack the uniquely favorable geometry of the Trapezium, background stars dominate the observed luminosity functions at the magnitudes of brown dwarfs, and hence the resulting constraints on the substellar IMF have large uncertainties.

To find promising candidates for low-mass stars and brown dwarfs in star-forming regions, several methods have been employed over the last decade. Because of the extreme youth of these objects, they can be identified via signatures of activity (X-rays), accretion ($H\alpha$, UV), and disks (mid-IR). Deep X-ray images are capable of detecting most of the low-mass stars in the nearest embedded clusters, but they reach few of the brown dwarfs (Feigelson & Lawson 2004; Scelsi et al. 2007; Stelzer, Micela & Neuhäuser 2004). Although $H\alpha$ imaging has not been used widely for this purpose, it did uncover some of the first spectroscopically-confirmed late-type members of star-forming regions (Comerón, Rieke & Neuhäuser 1999). As described earlier, mid-IR excess emission was used to identify GY141 as a possible disk-bearing brown dwarf. The ability of the *Spitzer Space Telescope* (Werner et al. 2004) to collect sensitive, wide-field mid-IR images has made it possible to apply this technique on a much larger scale (Allers et al. 2007, Luhman et al. 2009b, 2006, Muench et al. 2007, Rebull et al. 2010). Data from *Spitzer* have been particularly crucial for detecting heavily obscured, protostellar brown dwarfs (see Section 3.5).

As in open clusters, candidate low-mass members of star-forming regions also can be identified with proper motions and color-magnitude diagrams measured from optical and near-IR images. These data are generally more sensitive and unbiased than the surveys based on youth indicators. Proper motion selection of candidates has not been widely used in star-forming regions since extinction prevents many of the members from appearing in photographic plates. However, the earliest wide-field images with CCDs and near-IR detectors are growing old enough that sensitive proper motion surveys for low-mass members are becoming feasible. Such proper motion measurements are especially accurate if one or more epochs of images have been obtained with the *Hubble Space Telescope (HST)* given its high spatial resolution. Figure 1 shows an example of how *HST* can be used for this purpose. Ideally, if one could map the nearest star-forming regions with the resolution of *HST* and the wavelength coverage and sensitivity of *Spitzer* (e.g., *James Webb Space Telescope*) across a period of several years, virtually all of the members could be identified through proper motions.

Color-magnitude diagrams have proved to be the most successful tool for finding low-mass members of star-forming regions. Since clusters with ages of > 3 Myr usually have little extinction ($A_V < 2$), standard color-magnitude diagrams like those used for open clusters are sufficient for the selection of candidates. Examples of such populations include σ Ori (Béjar, Zapatero Osorio & Rebolo 1999), λ Ori (Barrado y Navascués et al. 2004), and Upper Sco (Slesnick, Carpenter & Hillenbrand 2006). However, extinction from the parent molecular cloud in younger regions can be quite large, and it varies significantly from one line of sight to another ($A_V = 0-$

50), which increases the contamination of reddened background stars in the area of a color-magnitude diagram inhabited by cluster members. Late-type members can be distinguished from these background stars by inspection of a color-color diagram like $I - K$ versus $J - H$ in which the reddening vector is roughly perpendicular to the sequence of dwarf colors (Luhman 2000). To represent the membership constraints from a color-magnitude diagram and $I - K$ versus $J - H$ more compactly, extinctions of individual stars can be estimated from the latter, which are then used to deredden the locations of stars in the color-magnitude diagram (Luhman et al. 2003a). The dramatic reduction in contamination from background stars is illustrated by the comparison of observed and extinction-corrected color-magnitude diagrams for Taurus in Figure 2. Thus, the most refined selection of candidate low-mass stars and brown dwarfs is produced when data at both optical and near-IR bands are available. 2MASS was an essential source of the IR data in early surveys, particularly in the larger regions like Taurus (Briceño et al. 2002). UKIDSS is now providing much deeper IR images for several nearby open and star-forming clusters (Lodieu, Hambly & Jameson 2006). Although the members of the most embedded clusters like Ophiuchus are often below the detection limits of optical images, it has been possible to identify candidate substellar members with JHK photometry alone (Alves de Oliveira et al. 2010). Specialized filters that are designed to measure the near-IR absorption bands from H_2O and CH_4 also have been used to search for cool members of star-forming regions (Burgess et al. 2009; Haisch, Barsony & Tinney 2010; Peña Ramírez et al. 2011). As in open clusters, candidates are usually confirmed through low-resolution optical or near-IR spectroscopy that demonstrates a late spectral type and a young age.

The nearest and richest stellar populations with ages of $\lesssim 10$ Myr are found in Taurus, Perseus (IC 348, NGC 1333), Chamaeleon, Orion (ONC, σ Ori, λ Ori), Ophiuchus, Lupus, and Upper Sco. Surveys of these regions have discovered a few hundred members that are likely to be brown dwarfs ($>M6$) with spectral types as late as early L (Lodieu et al. 2008, Luhman et al. 2009b, 2008, Weights et al. 2009, Zapatero Osorio et al. 2000). Candidate young T dwarfs also have been found in σ Ori (Zapatero Osorio et al. 2002, 2008) and Ophiuchus (Marsh, Kirkpatrick & Plavchan 2010). The membership of the former object is uncertain (Burgasser et al. 2004) while the source in Ophiuchus is too reddened for a foreground dwarf, seems too bright for a background dwarf, and does not match the spectra of normal T dwarfs, indicating that it may be a young member of the cloud. The samples of spectroscopically confirmed young low-mass stars and brown dwarfs in Taurus and Chamaeleon are particularly valuable because of their proximity, relatively low extinction, large sizes, lack of crowding and bright nebular emission, and the uniformity of their spectral classifications (Luhman 2008, Luhman et al. 2010, references therein). Upper Sco is also very promising; based on the number of known members above $\sim 0.5 M_\odot$, it should contain the largest substellar population of any star-forming region within 150 pc (> 200 brown dwarfs). Deep, wide-field surveys of Upper Sco through UKIDSS are beginning to realize its potential (Lodieu, Dobbie & Hambly 2011; Lodieu, Hambly & Jameson 2006; Lodieu et al. 2008).

2.5 Characterization of Stellar Properties

After a young low-mass star or brown dwarf is discovered, we can begin to study it in detail by estimating its basic stellar properties, such as its spectral type, effective temperature, extinction, bolometric luminosity, mass, and age. The methods for doing so are reviewed in this section. An extensive review of the characterization of older, cooler brown dwarfs can be found in Kirkpatrick (2005).

2.5.1 SPECTRAL TYPE The measurement of a spectral type is important for confirming that a given candidate is cool and young, and is not a field star or a galaxy. In addition, because low-mass stars and brown dwarfs are expected to maintain roughly constant temperatures during their early evolution, spectral types should comprise good observational proxies of stellar masses.

At ages of $\lesssim 100$ Myr, objects at the hydrogen burning mass limit are predicted to have temperatures near 3000 K (Baraffe et al. 1998, Burrows et al. 1997), corresponding to a spectral type of \sim M6. This prediction appears to be consistent with measurements of dynamical masses and Li abundances (Basri, Marcy & Graham 1996; Basri & Martín 1999; Close et al. 2007; Stassun, Mathieu & Valenti 2006, Sections 4.3). Young brown dwarfs should have progressively later types with decreasing mass, and could extend into the L and T spectral classes. For instance, evolutionary models predict that a brown dwarf with a mass of $2 M_{\text{Jup}}$ should have a temperature of ~ 1200 K at an age of 1 Myr, which corresponds to a spectral type of early T for field dwarfs (Kirkpatrick 2005). However, the onset of methane absorption (i.e., a type of T0) may occur at lower temperatures for young brown dwarfs than for older objects in the field (Barman et al. 2011b, Section 4.4).

The spectral types of field M and L dwarfs are defined by the strengths of various atomic and molecular absorption features (e.g., TiO, VO) that appear at red optical wavelengths (Henry, Kirkpatrick & Simons 1994; Kirkpatrick 2005; Kirkpatrick, Henry & Irwin 1997; Kirkpatrick, Henry & McCarthy 1991; Kirkpatrick et al. 1999a). Averages of optical spectra for dwarf and giant standards match well with the spectra of young late-M objects, and thus have been used to define the spectral types of these sources (Luhman 1999; Luhman, Liebert & Rieke 1997). Since L-type giants do not exist, a preliminary classification system for young L dwarfs has been defined at optical wavelengths based on a comparison to normal L dwarfs (Cruz, Kirkpatrick & Burgasser 2009). The standards for this scheme consist of nearby field dwarfs that have been identified as young based on their gravity sensitive lines (Cruz, Kirkpatrick & Burgasser 2009; Cruz et al. 2007; Kirkpatrick et al. 2006, 2008). L-type members of young clusters generally are less attractive as standards since they are fainter and can have significant reddening, although they do offer the advantage of known ages via their cluster membership. For field T dwarfs, the primary classification scheme is based on near-IR H₂O and C₂H₄ bands (Burgasser et al. 2006). The normal T dwarf standards are well-suited for classifying the moderately young T dwarf HN Peg B ($\tau \sim 300$ Myr, Luhman et al. 2007a). The classification of younger T dwarfs has not been explored since only a few candidates have been identified (Marsh, Kirkpatrick & Plavchan 2010; Zapatero Osorio et al. 2002).

Although their spectral types have been defined according to optical features, young late-M and L dwarfs are more easily observed at near-IR wavelengths, where they are brightest. To measure IR spectral types that are tied to the optical classification system, they should be based on 1) a comparison to dwarf standards for spectral features that do not depend on gravity or 2) a comparison to optically-classified sources with roughly the same age for features that depend on both grav-

ity and temperature (e.g., Cruz, Kirkpatrick & Burgasser 2009; Luhman 2008; Luhman et al. 2009b). Since the H₂O bands are the most prominent features in low-resolution near-IR spectra at M and L types, and since they do vary with both gravity and temperature, the latter approach is usually necessary. To illustrate this point, Figure 3 compares the spectra of an M6 member of Taurus, V410 X-ray 3, and a standard M6V field dwarf, Gl 406. The M6V dwarf matches the optical absorption bands but has weaker H₂O absorption. A much cooler field dwarf near L0V is required to reproduce the depth of H₂O in the low-gravity M6 object, as shown in Figure 3. Thus, using dwarfs as the standards for classifying young objects via their H₂O bands produces spectral types that are too late (Luhman et al. 2003b).

Gravity-sensitive spectral features like H₂O complicate the measurement of spectral types, but they also provide valuable constraints on the ages of late-type dwarfs. In particular, these features offer a means of confirming the youth, and hence the membership, of candidate low-mass members of young clusters and associations. Early surveys for young brown dwarfs used optical spectroscopy of Na I, K I, CaH, and VO for this purpose (Luhman, Liebert & Rieke 1997; Martín, Rebolo & Zapatero Osorio 1996; Steele & Jameson 1995), and similar features were soon recognized at near-IR wavelengths as well (Gorlova et al. 2003, Luhman et al. 1998). The variation of gravity-sensitive lines with age has been examined in detail in several studies (Kirkpatrick et al. 2006, McGovern et al. 2004, Rice et al. 2010), which have shown that differences of ~ 1 dex in $\log(\text{age})$ can be detected within a sample of objects (Kirkpatrick et al. 2008). This is illustrated in Figure 3, which compares transitions from Na I, K I, and FeH for late-M members of Taurus ($\tau \sim 1$ Myr), Upper Sco ($\tau \sim 12$ Myr Pecaut, Mamajek & Bubar 2012), and the field ($\tau \gtrsim 1$ Gyr). Spectral features of this kind have been used to define gravity classes that are denoted by the suffixes α , β , γ , and δ (e.g., L0 δ), which correspond roughly to ages of $\gtrsim 1$ Gyr, ~ 100 Myr, ~ 10 Myr, and ~ 1 Myr, respectively (Cruz, Kirkpatrick & Burgasser 2009; Kirkpatrick 2005; Kirkpatrick et al. 2006). Figure 3 also shows how the shape of the *H*-band continuum varies with gravity, exhibiting a broad plateau in old dwarfs and a triangular peak in young objects (Lucas et al. 2001). Because it can be detected in low-resolution spectra, this is a particularly useful gravity diagnostic.

To illustrate how the optical and near-IR SEDs of young low-mass objects vary with spectral type, Figure 4 shows low-resolution spectra of young sources from mid-M to early T. This sample consists of members of IC 348 (source 201, Luhman 1999), Taurus (V410 X-ray 3, Luhman et al. 1998), and TWA (2M 1207-3932 A and B, Chauvin et al. 2004, Gizis 2002), three young field dwarfs (2M 0141-4633, 2M 2208+2921, 2M 0355+1133, Cruz, Kirkpatrick & Burgasser 2009; Kirkpatrick et al. 2006), and the young companion HR 8799 b ($\tau \sim 60$ Myr, Marois et al. 2008). The spectral types of the earliest six sources were measured from optical spectra, but only near-IR spectra are available for 2M 1207-3932 B and HR 8799 b. The latter has been classified as early T based on the tentative detection of weak CH₄ absorption in the spectrum in Figure 4 (Barman et al. 2011a). Given its strong H₂O bands and its lack of CH₄, 2M 1207-3932 B is probably an L dwarf, but a more accurate classification has not been possible previously because it is much redder from 1–2 μm than normal L dwarf standards (Mohanty et al. 2007, Patience et al. 2010). As discussed at later points in this review, young L dwarfs like those in Figure 4 are also unusually red, which suggests that the red color of 2M 1207-3932 B is related to its youth. 2M 1207-3932 B closely matches the young L5 dwarf in Fig-

ure 4 from 1.4–2.5 μm , but is redder in the J -band, indicating that it is probably later than L5. Therefore, we adopt a type of L6–L9 for it. The spectral behavior of objects at very low masses and young ages like 2M 1207-3932 B and HR 8799 b will be discussed further in Section 4.4.

2.5.2 EFFECTIVE TEMPERATURE Effective temperatures of young low-mass objects have been estimated from spectral types and from fitting of spectral lines with the predictions of model atmospheres. For the first approach, a conversion between spectral types and temperatures is required. To develop a temperature scale that is appropriate for use with one of the most widely-used sets of evolutionary models (Baraffe et al. 1998), Luhman (1999) modified the scale for M dwarfs so that the components of the young quadruple system GG Tau (K7/M0.5/M5.5/M7.5, White et al. 1999) exhibit the same isochronal ages. Luhman et al. (2003b) then adjusted this scale further so that the sequences of IC 348 and Taurus at $\leq M9$ were parallel to those model isochrones on the Hertzsprung-Russell (H-R) diagram. The resulting scale may differ significantly from the true conversion, but in the absence of a robust determination of the temperature scale at young ages (e.g., eclipsing binaries), this scale offers a reasonable means of interpreting spectral types and luminosities in terms of masses and ages with evolutionary models. No attempt has been made to extend the temperature scale from Luhman et al. (2003b) to young L dwarfs since few of these objects have been found in young clusters, but it appears that they may have significantly different temperatures than dwarfs at a given spectral type (Section 4.4).

As an alternative to applying a temperature scale to spectral types, temperatures (and surface gravities) for young low-mass objects have been estimated by fitting absorption lines in high-resolution spectra with lines produced by model atmospheres (Mohanty, Jayawardhana & Basri 2004; Mohanty et al. 2004b; Rice et al. 2010). The resulting parameters are often consistent with the temperatures implied by spectral types and the gravities derived from evolutionary models, but their values do depend on the transitions in question and the adopted models. In addition, spectroscopy with sufficient resolution for detailed model fitting is feasible for only the brightest young brown dwarfs.

2.5.3 EXTINCTION Young brown dwarfs in the solar neighborhood have negligible extinction ($A_V < 0.5$), but members of star-forming regions are often obscured by their natal molecular clouds and (less frequently) circumstellar dust. Older stars in open clusters and associations also can have noticeable extinction ($A_V \sim 1$) if they are beyond the edge of the Local Bubble ($d \gtrsim 100$ pc). Estimating the amount of extinction toward young low-mass stars and brown dwarfs is necessary for measuring their bolometric luminosities. Reddening from extinction also must be considered during spectral classification since it significantly affects spectral slopes. Indeed, rather than use the slope to help constrain the spectral type, one typically must use it to estimate the extinction if significant obscuration is possible.

In early studies, extinctions for young low-mass stars and brown dwarfs were estimated by comparing their broad-band colors to the typical values for field dwarfs at a given spectral type. Samples of young objects are now large enough for types earlier than L0 that it has become possible to estimate their average intrinsic colors as a function of spectral type by assuming that the bluest sources at each spectral type have $A_V \sim 0$ (Luhman et al. 2010). Since they should

be unreddened, young M and L dwarfs in the solar neighborhood also have constrained the intrinsic colors at young ages (Cruz, Kirkpatrick & Burgasser 2009). Although colors are more widely used for estimating extinctions, the most accurate measurements are provided by the slopes of broad-coverage spectra (e.g., Figure 4) in comparison to unreddened standards.

2.5.4 BOLOMETRIC LUMINOSITY Many young low-mass stars and brown dwarfs lack photometry across a wide enough range of wavelengths for direct calculations of their bolometric luminosities. As a result, luminosities are usually estimated by applying bolometric corrections derived for field dwarfs to broad-band magnitudes, such as J , H , or K (Golimowski et al. 2004). This approach seemed reasonable since the near-IR colors of young M dwarfs are similar to those of field M dwarfs (Luhman 1999). However, beyond a spectral type of \sim M9, young objects become redder than their older counterparts in $J - K$ (Allers et al. 2010; Bihain et al. 2010; Briceño et al. 2002; Cruz, Kirkpatrick & Burgasser 2009; Faherty et al. 2009; Kirkpatrick et al. 2006, 2008; Schmidt et al. 2010). This trend is evident in a comparison of near-IR spectra of young L dwarfs like those in Figure 4 to spectra of field dwarfs, and it applies to the young planetary companions of HR 8799 as well (Marois et al. 2008), which probably have spectral types near the L/T transition (Barman et al. 2011a). Similarly, the colors between near- and mid-IR bands for young L dwarfs in the field are unusually red (Zapatero Osorio et al. 2010, 2011). The young T dwarf HN Peg B also exhibits red near- to mid-IR colors, although its near-IR colors are normal (Luhman et al. 2007a). Thus, the bolometric corrections for young L and T dwarfs are probably not the same as those for standard field dwarfs. As a result, luminosities based on dwarf-like bolometric corrections are probably underestimated, which may partially explain why young L dwarfs are underluminous compared to normal dwarfs in near-IR bands (Faherty et al. 2012) and why the sequences of young clusters on H-R diagrams are underluminous relative to model isochrones at the latest types (Luhman et al. 2008, Section 4.4). Near- and mid-IR data are now available for a sufficiently large number of young low-mass objects that one could estimate the typical bolometric corrections as a function of spectral type at young ages, but this has been done only for a few specific spectral types to date (Todorov, Luhman & McLeod 2010; Zapatero Osorio et al. 2010).

2.5.5 MASS AND AGE Masses and ages for young low-mass stars and brown dwarfs are normally estimated by comparing their temperatures and luminosities to the values predicted by theoretical evolutionary models (Section 4.4). The estimates for a given object depend significantly on the details of this process, such as the adopted temperature scale and evolutionary models, but it is possible to arrive at masses and ages for young M dwarfs that are roughly consistent with measurements of dynamical masses, the expected coevality of components of multiple systems, and other observational constraints (Luhman & Potter 2006). However, the errors in these masses and ages are likely rather high at L and T types where the SEDs are peculiar and the atmospheric models are more uncertain. As a result, whenever possible, it is preferable to discuss young low-mass objects in terms of observational parameters that are likely to be correlated with mass and age, namely spectral types and gravity-sensitive spectral lines (Section 3.2, 4.4).

3 FORMATION AT LOW MASSES

3.1 Theory

Several mechanisms have been proposed for the formation of low-mass stars and brown dwarfs (Bonnell, Larson & Zinnecker 2007; Whitworth et al. 2007). They can be summarized as follows:

1. Gravitational compression and fragmentation of gas in a massive collapsing core produces fragments over a wide range of masses. The tidal shear and high velocities within the cluster prevent the low-mass objects from accreting to stellar masses (Bonnell, Clark & Bate 2008).
2. Dynamical interactions among fragments or protostars in a massive core lead to the ejection of some of them from the core, which prematurely halts their accretion (Bate 2009; Bate & Bonnell 2005; Bate, Bonnell & Bromm 2002, 2003; Boss 2001; Goodwin, Whitworth & Ward-Thompson 2004; Reipurth & Clarke 2001; Umbreit et al. 2005).
3. Instead of ejection, photoionizing radiation from OB stars halts accretion by removing much of the envelope and disk of a low-mass protostar (Hester et al. 1996, Whitworth & Zinnecker 2004).
4. The gravitational fragmentation of massive circumstellar disks around stars produces low-mass companions. Some of these objects are ejected through dynamical interactions with other companions or nearby stars (Bate & Bonnell 2005; Bate, Bonnell & Bromm 2002, 2003; Goodwin & Whitworth 2007; Offner, Klein & McKee 2008; Offner et al. 2009; Rice et al. 2003; Shen et al. 2010; Stamatellos, Hubber & Whitworth 2007; Stamatellos & Whitworth 2009; Stamatellos et al. 2011; Thies et al. 2010; Whitworth & Stamatellos 2006).
5. Turbulent compression and fragmentation of gas in a molecular cloud produces collapsing cores over a wide range of masses (Elmegreen 2011, Hennebelle & Chabrier 2008, Padoan & Nordlund 2002, 2004). The mass of each core determines the mass of the resulting star. Low-mass stars and brown dwarfs arise from the smallest cores.

Observations of low-mass stars and brown dwarfs that can potentially be used to test these theories include the shape of the low-mass IMF and its minimum mass, stellar multiplicity, spatial and kinematic distributions at birth, the prevalence and sizes of circumstellar disks and envelopes, and the dependence of these properties on star-forming environment. The number and specificity of predictions for comparison to these data vary considerably among the models. Reipurth & Clarke (2001) and Bate, Bonnell & Bromm (2002, 2003) have led in this respect, providing valuable motivation for a wide range of observational studies over the last decade. Unfortunately, when available, some of the predictions for a given property are rather similar, limiting the ability of observations to discriminate among models. For instance, nearly all of the newer models predict that the velocities of newborn stars and brown dwarfs are indistinguishable, that brown dwarfs have low binary fractions, and that the IMF is roughly log-normal with a characteristic mass of $\sim 0.5 M_{\odot}$. In addition, although published values for the minimum mass for opacity-limited fragmentation range from 0.001–0.01 M_{\odot} (Bate & Bonnell 2005; Bate, Bonnell & Bromm 2002; Boss 1988; Boyd & Whitworth 2005; Low & Lynden-Bell 1976; Rees 1976; Silk 1977; Whitworth & Stamatellos 2006;

Whitworth et al. 2007), a given set of models is often consistent with a fairly wide range of values. The dependence of the minimum mass on star-forming conditions may represent a better test of the models, but the number statistics available in young clusters will limit the accuracy of such measurements. Predictions do differ significantly for the frequency of wide binaries, the distribution of binary eccentricities, the ability of brown dwarfs to form in isolation, and the formation and survival of protostellar brown dwarfs. In the remainder of this section, we review the current observational constraints on these properties and the others mentioned above, and compare them to theoretical predictions.

3.2 Initial Mass Function

In this section, we summarize measurements of the IMF of low-mass stars and brown dwarfs in the solar neighborhood and the nearest young clusters and discuss the insight they provide into the formation of these objects. Bastian, Covey & Meyer (2010) also have described some of these studies as a part of a larger review of evidence for variations in the IMF.

3.2.1 SOLAR NEIGHBORHOOD AND GALACTIC DISK Measurements of the IMF are frequently characterized in terms of the power-law forms $dN/dM \propto M^{-\alpha}$ or $dN/d\log M \propto M^{-\Gamma}$, where $\alpha = \Gamma + 1$ and the Salpeter value is $\alpha = 2.35$. The mass function of stars in the solar neighborhood and the Galactic disk has been found to rise with a roughly Salpeter slope down to $\sim 0.5 M_{\odot}$, where it then flattens by $\Delta\alpha \sim 1.5$ (Bochanski et al. 2010; Chabrier 2001; Covey et al. 2008; Deacon, Nelemans & Hambly 2008; Kroupa 2002; Reid, Gizis & Hawley 2002). Similar IMFs have been measured in young clusters, as discussed in the next section.

Since the photometric properties of field brown dwarfs are distinct from those of most low-mass stars, their mass function has been estimated through a separate set of surveys. Based on L and T dwarfs uncovered by wide-field surveys like 2MASS, SDSS, and UKIDSS, the substellar mass function in the solar neighborhood exhibits a slope of $\alpha \sim 0$ (Allen, Koerner & Reid 2005; Burningham et al. 2010; Chabrier 2002; Metchev et al. 2008; Pinfield et al. 2008; Reid et al. 1999; Reyl e et al. 2010). In comparison, slopes reported for young clusters tend to be near $\alpha \sim 0.5$ (Section 3.2.2). This difference is probably not significant since the substellar mass functions in the field and clusters have been derived with different methods and thus are subject to different systematic errors. There is no evidence of the surplus of brown dwarfs in the field compared to young clusters that is expected if brown dwarfs are born with much higher space velocities than stars (Kroupa & Bouvier 2003, Moraux & Clarke 2005).

The recent all-sky mid-IR imaging survey by the Wide-field Infrared Survey Explorer (WISE, Wright et al. 2010) offers an opportunity to further improve measurements of the substellar mass function in the field. Data from WISE have already been used to discover ~ 100 late T dwarfs (Kirkpatrick et al. 2011) and objects at even cooler temperatures, known as Y dwarfs (Cushing et al. 2011, $T_{\text{eff}} < 500$ K). Brown dwarfs at $T_{\text{eff}} \lesssim 300$ K are particularly valuable since their numbers are sensitive to minimum masses of the IMF in the range of $5\text{--}10 M_{\text{Jup}}$ (Burgasser 2004, Kirkpatrick et al. 2011). Only ~ 1 field brown dwarf of this kind has been found to date, but the WISE surveys are still ongoing and the statistical constraints on the minimum of the IMF should improve.

3.2.2 YOUNG CLUSTERS The surveys for low-mass stars and brown dwarfs in young open clusters and star-forming regions described in Sections 2.3 and 2.4 have produced a large number of IMF measurements (e.g., Barrado y Navascués, Stauffer & Jayawardhana 2001; Béjar et al. 2001; Briceño et al. 2002; Lodieu, Dobbie & Hambly 2011; Moraux, Kroupa & Bouvier 2004; Slesnick, Hillenbrand & Carpenter 2008). Most of the estimated IMFs are fairly similar with $\alpha \sim 0.5$ at $M \lesssim 0.2 M_{\odot}$. There have been a few reports of variations among these data, but reliably detecting IMF variations requires that all of the IMFs subject to comparison have been 1) derived with the same evolutionary models, spectral classification system, and temperature scale, 2) assessed rigorously for completeness, and 3) measured from large enough fields to avoid effects of mass segregation. Claims of variations in low-mass IMFs also should be treated with skepticism unless they are evident in a direct comparison of the data (e.g., spectral types) on which the IMFs are based. Given these considerations, we find that the only significant variation in published low-mass IMFs is the unusually high peak mass in Taurus (Briceño et al. 2002, Luhman et al. 2003b). This variation is illustrated in Figure 5, which shows a comparison of spectral type distributions for representative samples of members of Taurus, IC 348, and Chamaeleon I (Luhman 2007, Luhman et al. 2009b, 2003b). The distributions in IC 348 and Chamaeleon I peak at M5 while Taurus exhibits a large surplus of K7–M1 stars ($\sim 0.8 M_{\odot}$). It would be quite interesting to measure distributions of spectral types with the same classification system and comparable completeness for additional clusters. Because of the narrow widths of the peaks at M5 in IC 348 and Chamaeleon I, it should be possible to detect fairly small variations in the spectral type of this peak (i.e., the IMF’s characteristic mass) when comparing clusters at similar ages. In addition, a comparison of clusters across a range of ages (e.g., IC 348 vs. the Pleiades) could reveal how spectral type evolves with age for the mass corresponding to the maximum of the IMF, assuming that the IMF is invariant within the sample of clusters. Currently, the available spectral types for low-mass members of most clusters are not sufficiently numerous, representative, or uniformly measured for these experiments.

The samples from Figure 5 for Taurus and Chamaeleon I are shown in terms of IMFs in Figure 6, which have been derived with the evolutionary models of Baraffe et al. (1998) and Chabrier et al. (2000b). We also include mass functions for the Pleiades (Moraux, Kroupa & Bouvier 2004) and the field (Bochanski et al. 2010, see Section 3.2.1). As implied by the distributions of spectral types, the IMF in Taurus peaks at a higher mass than the IMF in Chamaeleon I and other young clusters. Meanwhile, the mass function in Chamaeleon I is roughly similar to those in the Pleiades and the field. It is not possible to attribute small differences between Chamaeleon I, the Pleiades, and the field to true variations in the IMF since each population is subject to different systematic errors. Previous explanations for the unusually high peak mass in Taurus have generally involved a higher average Jeans mass compared to other regions (Briceño et al. 2002; Goodwin, Whitworth & Ward-Thompson 2004; Lada et al. 2008; Luhman 2004c; Luhman et al. 2003b). A recent numerical simulation of the formation of both distributed and clustered stars has also reproduced the variations in peak mass between Taurus and other clusters (Bonnell et al. 2011). However, the width of the IMF is predicted to be more narrow in a distributed population than in clusters, whereas the IMF in Taurus is as broad as IMFs in other regions. This suggests that the breadth of the IMF is not caused by dynamical interactions. As discussed in Sections 2.3, 2.4, and 3.2.1, surveys in the field and in young clusters

indicate that the IMF extends down to at least $0.01 M_{\odot}$. A small number of objects have been identified that may have even lower masses, but they have uncertain masses and sometimes are poorly characterized in terms of spectral type and age. Thus, current data are insufficient for a stringent test of the predictions of the minimum mass of the IMF.

To search for variations in the substellar mass function, the ratio of the number of brown dwarfs to the number of stars is often compared among young clusters (Briceño et al. 2002, Luhman et al. 2003b). However, this ratio is probably not a reliable diagnostic of such variations (Luhman 2007). Because of the close proximity of the IMF's peak to the hydrogen burning limit, the brown dwarf ratio is sensitive to true variations in the peak mass (which would not provide any specific insight into brown dwarfs) and false variations that stem from different choices of evolutionary models, mass indicators (photometry vs. spectral type), spectral classification schemes, and temperature scales. This ratio also can depend on field size within a cluster because of mass segregation (Muench et al. 2003). Instead, it is better to characterize the low-mass IMF by its slope from the peak down to the completeness limit when comparing results from different studies since it is less susceptible to these systematic differences in mass estimates. As noted above, no significant variations in these slopes are apparent in published IMFs for young clusters ($N_{BD}/N_{star} \sim 0.2$, Andersen et al. 2006; Luhman 2007; Slesnick, Hillenbrand & Carpenter 2004, references therein). Since the mass function of brown dwarfs is roughly the same regardless of the presence of O stars, we can conclude that halting of accretion by photoionizing radiation is not the dominant process that results in the formation of brown dwarfs. Similarly, Taurus has a very low stellar density, and yet it has produced a comparable abundance of brown dwarfs as much denser clusters like the Trapezium, indicating that dynamical interactions are not essential for the formation of brown dwarfs. If brown dwarfs form predominantly in disks around solar-type stars, then the numbers of brown dwarfs and solar-type stars should scale together, but this is not seen in the comparison of Taurus to other clusters. Indeed, given the paucity of solar-mass ($\sim K7$) stars in most clusters (e.g., see IC 348 in Figure 5), it seems unlikely that their disks have hosted the formation of a large fraction of low-mass stars and brown dwarfs.

Finally, we note that the mass functions of pre-stellar cores in molecular clouds resemble the stellar IMF in terms of the Salpeter slope at high masses and the flattening at low masses, which has been taken as evidence that gravitational or turbulent fragmentation determines the masses of stars, and perhaps brown dwarfs (André et al. 2010, Rathborne et al. 2009, references therein). However, whether a physical relationship truly exists between these mass functions remains a subject of debate (e.g., Chabrier & Hennebelle 2010; Michel, Kirk & Myers 2011; Smith, Clark & Bonnell 2009).

3.3 Multiplicity

The properties of multiple systems are influenced by both the process of star formation and dynamical interactions within and among stellar systems. Thus, measurements of multiplicity may shed light on the formation and early evolution of low-mass stars and brown dwarfs. Since this topic has been reviewed by Burgasser et al. (2007), we will focus on the new results since that review and the implications of the observed multiplicity properties for the proposed formation mechanisms.

Multiplicity at low masses has been studied in both the solar neighborhood and in young clusters. Each of the two populations has advantages. Binary properties can be measured down to smaller separations in the field while the youngest clusters allow us to characterize the primordial multiplicity properties and their dependence on star-forming conditions. For field stars and brown dwarfs, the binary fractions and average separations decrease and the average mass ratios increase ($q \equiv M_2/M_1$) at lower primary masses (e.g., Basri & Reiners 2006, Bergfors et al. 2010, Bouy et al. 2003, Burgasser et al. 2003, Close et al. 2003, Duquennoy & Mayor 1991, Fischer & Marcy 1992, Figure 7). The change in these properties with mass appears to be continuous rather than abrupt (e.g., Kraus & Hillenbrand 2012), resembling the behavior of the IMF, accretion rates, and disk fractions (Sections 3.2, 3.4). Based on analysis by Burgasser et al. (2003), it is unlikely that wide low-mass binaries have been disrupted while in the field, and instead the paucity of these systems is probably primordial or caused by dynamical interactions at very young ages ($\tau \lesssim 10$ Myr). We can attempt to distinguish between these two possibilities by examining the multiplicity of low-mass members of nearby star-forming regions that have low stellar densities so that dynamical effects are minimized. The best available options are Taurus and Chamaeleon I. High-resolution imaging of the members of these regions has found that the frequency of wide binaries and their average separation decrease steadily from solar-mass stars to brown dwarfs (Konopacky et al. 2007; Kraus & Hillenbrand 2007, 2009a, 2012; Kraus et al. 2011b; Kraus, White & Hillenbrand 2006; Lafrenière et al. 2008; Neuhäuser et al. 2002, K. Todorov, in preparation). The trend at low masses is illustrated in Figure 7, where we plot the separations for binaries and the limits for unresolved sources versus spectral type from M4 to L0. The observed binary fractions from these data are 13/62 ($21^{+6}_{-4}\%$) for M4–M6 and 5/74 ($7^{+4}_{-2}\%$) for $>M6$, which apply to separations of > 5 –10 AU. Although the average separation decreases with later types, a few very wide systems (> 100 AU) are present at $>M6$ (Luhman 2004a, Luhman et al. 2009a). Therefore, we conclude that part of the dependence of multiplicity on primary mass observed in the field is primordial, but dynamical interactions in denser clusters are probably also responsible for the small frequency of very wide binaries in the field. The role of environment can be examined by considering additional star-forming regions. For instance, based on data similar to those obtained in Taurus and Chamaeleon I, members of Upper Sco later than M6 have an observed binary fraction of 0/22 ($< 8\%$, Biller et al. 2011; Kraus, White & Hillenbrand 2005). This measurement is lower than the value in Taurus, but the difference is not statistically significant.

It would be desirable to closely compare multiplicity measurements between the field and star-forming regions to search for signs of dynamical evolution at ages of $\gtrsim 10$ Myr. For such a comparison to be meaningful, the selected star-forming region should be representative of the birth places of most field stars. It is likely that the field has been populated predominantly by moderately rich clusters ($N > 100$) within giant molecular clouds that become OB associations (e.g., Orion, Upper Sco) rather than small, loose aggregates (e.g., Taurus, Lada & Lada 2003). However, the number statistics for the low-mass binary measurements in Upper Sco are too low for a detailed comparison to the field, and measurements in dense clusters like the ONC are hampered by chance alignments of unrelated stars.

A few sets of formation models have made specific predictions for the binary properties of brown dwarfs. We can compare those predictions to observations, which can be summarized as follows based on the field and cluster

data: brown dwarfs have a binary fraction of 20–30% (Basri & Reiners 2006, Maxted & Jeffries 2005), most of the binaries are tight (<20 AU) and a few are very wide > 100 AU, and the mass ratios tend to approach unity. Early models produced too few binaries and no wide systems (Bate, Bonnell & Bromm 2002; Reipurth & Clarke 2001) but newer calculations are roughly consistent with the data (Bate 2009, 2012, Bate & Bonnell 2005, Stamatellos & Whitworth 2009). The trends in mass ratio and mean separation as a function of stellar mass are also qualitatively reproduced by Bate (2009, 2012). However, it remains unclear whether any of these models can make wide binary brown dwarfs in the low-density conditions in which they have been primarily found. The binary FU Tau (800 AU, Luhman et al. 2009a) and the quadruple containing 2MASS 04414489+2301513 (1700 AU, Todorov, Luhman & McLeod 2010) would seem difficult to explain with dynamical or disk fragmentation models given that they are both fragile and isolated. Finally, the distribution of eccentricities predicted by Bate (2009) is consistent with data for low-mass binaries in the field while the binaries from Stamatellos & Whitworth (2009) are weighted too heavily toward high eccentricities (Dupuy & Liu 2011, Konopacky et al. 2010). However, the initial orbital properties from these models could be altered by dynamical interactions, making it difficult to conclusively test formation scenarios with data from old binaries in the field.

3.4 Circumstellar Disks

Newborn stars experience much of their growth via accretion from circumstellar disks, and it has been proposed that brown dwarfs arise when this accretion is prematurely halted. As a result, observations of accretion and disks around young low-mass stars and brown dwarfs may prove useful in understanding their formation. As with multiplicity, this topic was reviewed in *Protostars and Planets V* (Luhman et al. 2007d), so we will provide a summary of the observations that includes the latest results, and describe the implications for the formation theories.

In the model of magnetospheric accretion, matter from a circumstellar disk falls onto a young star along its magnetic field lines. The impact of the material onto the stellar surface produces an accretion shock, which radiates at UV and optical wavelengths. The columns of material accreting onto a young star also emit hydrogen emission lines that are significantly stronger and broader than those from stellar chromospheres, offering an additional tracer of accretion. Because H α is more easily observed in brown dwarfs than UV emission, line profiles of H α provided the first evidence of accretion for young low-mass objects (Jayawardhana, Mohanty & Basri 2002; Muzerolle et al. 2000). Additional accretion diagnostics have included Ca II (Mohanty, Jayawardhana & Basri 2005), near-IR hydrogen transitions (Natta et al. 2004), and optical continuum veiling (White & Basri 2003). Although they are more difficult to collect, measurements of UV excess emission have produced the most direct estimates of accretion rates (Herczeg & Hillenbrand 2008). The resulting rates are correlated with those derived from H α , but are systematically larger by a factor of several. The accretion rates from these various diagnostics are correlated with stellar mass as $\dot{M} \propto M^2$ for the full range of masses across which they have been measured ($M \sim 0.02\text{--}2 M_{\odot}$, Herczeg & Hillenbrand 2008; Mohanty, Jayawardhana & Basri 2005; Muzerolle et al. 2005; Natta, Testi & Randich 2006), although it has been sug-

gested that this apparent correlation may be largely due to selection effects (Clarke & Pringle 2006). If a dependence on stellar mass is present, its origin is unclear (Hartmann et al. 2006, Vorobyov & Basu 2009). Accretion rates in low-mass objects (and young stars in general) exhibit significant variability, which explains some of the scatter in the correlation between accretion rate and stellar mass (Scholz & Jayawardhana 2006). As with stars, outflows should be a natural byproduct of accretion onto brown dwarfs. Evidence of outflows from brown dwarfs has been detected in the form of emission in optical forbidden lines and blue shifted absorption in permitted lines (Fernández & Comerón 2001; Mohanty, Jayawardhana & Basri 2005; Muzerolle et al. 2005; White & Hillenbrand 2004). A few of these outflows have been spatially resolved through spectro-astrometry of the forbidden lines (Whelan et al. 2005, 2009) and submillimeter interferometry of CO emission (Phan-Bao et al. 2008, 2011). Outflows also have been observed in low-mass protostars, as discussed in Section 3.5.

Circumstellar disks around young stars can be studied via their thermal and line emission at IR and millimeter wavelengths where they dominate the stellar photosphere. Some of the earliest detections of disks around young objects near and below the hydrogen burning limit were achieved through photometry at 2–3 μm (Jayawardhana et al. 2003; Liu, Najita & Tokunaga 2003; Luhman 1999; Muench et al. 2000). However, because of their low luminosities, most low-mass stars and brown dwarfs do not heat their disks sufficiently for significant excess emission to appear at those wavelengths (Luhman et al. 2010). As a result, photometry at longer, mid-IR wavelengths is necessary for reliable detections of these relatively cool disks. The *Infrared Astronomical Satellite* (IRAS) measured mid-IR photometry for a few low-mass stars in sparse regions like Taurus (Kenyon & Hartmann 1995) and similar data were collected for some of the brightest young brown dwarfs by *ISO* (Comerón et al. 1998, Natta et al. 2002) and large ground-based telescopes (Apai et al. 2004, Sterzik et al. 2004). The arrival of the *Spitzer Space Telescope* resulted in a breakthrough in surveys for disks around brown dwarfs (as well as stars in general). The unprecedented mid-IR sensitivity of *Spitzer* enabled detections of disks around the faintest and coolest known members of the nearest star-forming regions (Luhman et al. 2005b). In addition, it could perform these measurements for nearly all of the members of these regions because of its ability to efficiently map large areas of sky (Luhman et al. 2010, references therein). The data from *Spitzer* have been used to measure the fraction of stars and brown dwarfs that harbor inner disks as a function of spectral type, which acts as a proxy for stellar mass. Figure 8 shows some of the best available disk fractions in terms of number statistics and completeness at low masses, which apply to Taurus, Chamaeleon I, and IC 348 (Lada et al. 2006, Luhman et al. 2005a, 2008, 2010, Muench et al. 2007). We also include new disk fractions for Upper Sco based on WISE photometry (K. Luhman, in preparation, see also Carpenter et al. 2006). In these data, disks remain common in star-forming regions down to the least massive known members ($\sim 0.01 M_{\odot}$). In fact, the evolution of these disk fractions with age from the youngest to oldest region indicates that the lifetimes of disks around low-mass stars and brown dwarfs are longer than those of more massive stars. The first hints of the potential longevity of disks at low stellar masses were provided by the detections of disks around two of the brown dwarfs in TWA (Mohanty, Jayawardhana & Barrado y Navascués 2003; Morrow et al. 2008; Riaz & Gizis 2008; Sterzik et al. 2004).

A number of studies have sought to characterize the physical properties of

the circumstellar disks identified in the *Spitzer* surveys. The radii of most disks around young stars cannot be directly measured with current technology. However, if a disk is viewed nearly edge-on, it can occult the star and be detected in scattered light. Using a combination of *Spitzer* spectroscopy and high-resolution imaging from *HST*, Luhman et al. (2007c) detected an edge-on disk around a young brown dwarf in Taurus and were able to estimate a disk radius of 20–40 AU. SEDs of young stars do not normally provide good constraints on disk radii because of degeneracies between radius and other parameters in disk models, but the circumprimary disk of the brown dwarf 2MASS J04414489+2301513 appears to be so small ($R = 0.2\text{--}0.3$ AU) that the degeneracies are minimal (Adame et al. 2011). The small size of this disk may be due to truncation by its secondary ($M \sim 5\text{--}10 M_{\text{Jup}}$, $a = 15$ AU, Todorov, Luhman & McLeod 2010). No other measurements of disk radii are available for young brown dwarfs. Masses have been measured for small samples of young low-mass objects through far-IR and millimeter observations (Harvey et al. 2011; Klein et al. 2003; Mohanty et al. 2012; Scholz, Jayawardhana & Wood 2006), which have produced values of $\lesssim 1 M_{\text{Jup}}$ assuming a standard gas-to-dust ratio of 100. Based on modeling of SEDs, the geometries of brown dwarf disks range from flared to relatively flat (Apai et al. 2004, Mohanty et al. 2004a, Natta & Testi 2001), which are believed to correspond to varying degrees of dust grain growth and settling. *Spitzer* spectroscopy of the $10 \mu\text{m}$ silicate emission feature has provided direct evidence of dust processing and the production of crystalline grains (Apai et al. 2005, Furlan et al. 2005). The silicate feature is weaker at later spectral types (Furlan et al. 2011, Kessler-Silacci et al. 2007, Morrow et al. 2008, Scholz et al. 2007), indicating that grain growth may occur faster in disks around brown dwarfs than in disks around stars. The disks of low-mass stars and brown dwarfs may also differ from those of solar-type stars in terms of their abundances of organic molecules (Pascucci et al. 2009). The evolution of disks may depend on stellar mass as well; disks with inner holes, known as transitional disks, have been uncovered around low-mass objects (Furlan et al. 2011, Muzerolle et al. 2006), but it appears that they are less common at lower stellar masses (Muzerolle et al. 2010).

In all of the proposed formation mechanisms from Section 3.1, brown dwarfs harbor accretion disks when they are born. Some of the models suggest that brown dwarfs have low masses because dynamical interactions ended accretion early, but few concrete predictions have been made regarding disk properties. As a result, all of the models are technically consistent with all of the observations of brown dwarf disks, such as the continuity of accretion rates and disk fractions from solar-type stars to brown dwarfs. The ejection models do predict that brown dwarf disks will have radii of $\lesssim 10$ AU (Bate, Bonnell & Bromm 2003), but they allow for a few somewhat larger disks (Bate 2009), and thus are consistent with the 20–40 AU disk in the edge-on system mentioned above. The measurements of disks around low-mass stars and brown dwarfs described in this section provide valuable constraints on the stellar mass dependence of the physics of accretion, disk evolution, and planet formation, but unfortunately they have not offered direct tests of the possible formation mechanisms for brown dwarfs.

3.5 Protostars

All of the proposed formation mechanisms for brown dwarfs occur during either cloud fragmentation or the protostellar phase. Thus, observations of the

youngest progenitors of low-mass stars and brown dwarfs should provide direct constraints on the formation models. For instance, brown dwarfs that form by disk fragmentation or ejection should never appear as isolated protostars.

A defining characteristic of a protostar is the presence of both an accretion disk and an infalling envelope. Protostars are often designated as class 0 or class I based on their SEDs, where class 0 is redder and presumably less evolved than class I (André, Ward-Thompson & Barsony 1993; Lada 1987). The all-sky mid-IR data from IRAS enabled the first comprehensive surveys for protostars, which uncovered a few class I candidates with spectral types as late as $\sim M5$ ($M \sim 0.15 M_{\odot}$), such as IRAS 04158+2805, IRAS 04248+2612, and IRAS 04489+3042 in Taurus (Kenyon & Hartmann 1995). The class I nature of these objects has been confirmed by the detections of envelopes (Andrews et al. 2008, Furlan et al. 2008, White & Hillenbrand 2004). High-resolution images from *HST* of the protostar IRAS 04325+2402 have revealed a faint nebulous companion that could be a class I brown dwarf (Hartmann et al. 1999, Scholz et al. 2008), although confirmation via mid-IR observations is not currently possible because of its small separation from the primary.

To identify free-floating protostellar brown dwarfs, sensitive wide-field mid-IR images are necessary, and the first data of this kind became available via the *Spitzer Space Telescope*, as mentioned previously in this review. Surveys for low-mass protostars have been conducted by either obtaining *Spitzer* images of samples of molecular cloud cores, often selected based on the absence of previously detected stars (“starless” cores), or searching for candidate protostars anywhere in the *Spitzer* images of a star-forming region regardless of the availability of previous detections of cores (Dunham et al. 2008). In both cases, the candidates must be confirmed as protostars associated with the target molecular cloud. For class 0 sources, a commonly employed signature of cloud membership is the presence of an outflow (Bourke et al. 2005). Since they have less obscuration, class I candidates are often bright enough at near-IR wavelengths for spectroscopy to verify that they are young brown dwarfs rather than galaxies (Luhman & Mamajek 2010). It is also necessary to detect the envelopes of class I objects since the SEDs of class II sources (star+disk) can resemble class I SEDs if they are highly reddened, as in the case of the Taurus brown dwarf 2MASS J04194657+2712552 (Furlan et al. 2011, Luhman et al. 2009b). To date, *Spitzer* surveys have identified more than a dozen candidate class 0 sources with luminosities that are indicative of young brown dwarfs ($L < 0.1 L_{\odot}$, Dunham et al. 2008), several of which have been confirmed as protostellar (Bourke et al. 2006, Dunham et al. 2006, 2010, Kauffmann et al. 2011, Lee et al. 2009, Young et al. 2004). Some of these objects may eventually accrete enough to become stars (Dunham et al. 2010) while others seem destined to remain substellar given their small accretion reservoirs (Lee et al. 2009). The existence of isolated protostellar brown dwarfs would indicate that the dynamical interactions, fragmentation in disks, and photoionizing radiation from massive stars are not essential for the formation of free-floating brown dwarfs.

3.6 Kinematics and Positions at Birth

Since dynamical interactions play a central role in some of the proposed formation mechanisms for low-mass stars and brown dwarfs, the observed kinematic and spatial distributions of these objects can provide tests of the models. For instance,

some of the earlier ejection models predicted that brown dwarfs are born with higher velocities than stars (Kroupa & Bouvier 2003, Reipurth & Clarke 2001).

Radial velocities have been measured for only small samples of late-type members of star-forming regions, but the available data indicate that young stars and brown dwarfs have similar velocity dispersions (Joergens 2006; Joergens & Guenther 2001; Kurosawa, Harries & Littlefair 2006; White & Basri 2003). Brown dwarfs also share the same spatial distributions as stars in Taurus and Chamaeleon I, whereas they should be more widely distributed if they are born with higher velocities (Guieu et al. 2006; Luhman 2006, 2007; Parker et al. 2011; Slesnick, Carpenter & Hillenbrand 2006). These results are consistent with most of the latest theories for the formation of brown dwarfs.

Both the ejection models and the disk fragmentation models require the presence of stars to produce brown dwarfs since stars facilitate the dynamical interactions that lead to ejection and act as the hosts of the fragmenting disks. As a result, it should not be possible for brown dwarfs to form in isolation if either of these mechanisms is required for their formation. Taurus is the best site for identifying brown dwarfs that are likely to have been born alone, and thus testing this prediction, since it is one of the richest nearby star-forming regions (~ 400 members) as well as one of the most sparsely distributed ($n \sim 1-10 \text{ pc}^{-3}$). The components of the wide binary FU Tau are the clearest examples of brown dwarfs in Taurus that have been born in relative isolation (Luhman et al. 2009a). They are projected against the center of the Barnard 215 dark cloud, which is their likely birth place. Only one other known member of Taurus, FT Tau, is found within 0.5° of this system. The fact that FU Tau A and B were born in the absence of stars indicates that dynamical processes and disk fragmentation played no role in their formation. The probable protostellar brown dwarfs described in Section 3.5 also have few neighboring stars and may be younger analogs of FU Tau.

4 EARLY STELLAR EVOLUTION AT LOW MASSES

4.1 Theory

The early evolution of low-mass stars and brown dwarfs ($\tau \lesssim 100 \text{ Myr}$) can be characterized largely in terms of the change in bolometric luminosity, effective temperature, radius, and angular momentum over time for a given stellar mass. Theoretical models of stellar interiors and atmospheres have made predictions for the evolution of the first three parameters while other structures (e.g., winds, disks) may lead to loss of angular momentum. The basic ingredients of modern evolutionary and atmospheric models for low-mass stars and brown dwarfs have been reviewed by Allard et al. (1997) and Chabrier & Baraffe (2000). Over the last decade, the possible effects of additional processes have been explored and some of the major results can be summarized as follows:

1. Magnitudes and colors produced by evolutionary models are sensitive to uncertainties in molecular line lists and opacities, but luminosities and temperatures are not affected significantly (Baraffe et al. 2002).
2. Evolutionary tracks on the H-R diagram for a given mass are sensitive to the initial radius for ages of $\lesssim 1 \text{ Myr}$ (Baraffe et al. 2002).
3. The predicted temperature for a given mass and age and the change in

temperature over time (i.e., verticality of mass tracks) depend on the choice of mixing length, particularly at younger ages (Baraffe et al. 2002)

4. The radius and luminosity may be influenced by previous episodes of intense accretion for ages up to ~ 10 Myr. The direction of this change is determined by whether thermal energy from the accreting matter is added to the star (Baraffe, Chabrier & Gallardo 2009; Hartmann, Cassen & Kenyon 1997; Hosokawa, Offner & Krumholz 2011).
5. The presence of strong magnetic fields and heavily spotted surfaces may result in a larger radius and a cooler temperature (Chabrier, Gallardo & Baraffe 2007; MacDonald & Mullan 2009).
6. Unstable modes with timescales of 1–5 hours may occur during deuterium burning (Palla & Baraffe 2005).

To test the accuracy of the standard models for the early evolution of low-mass objects in light of the above possible complications, we describe in this section observational constraints on the evolution of angular momentum, temperature, luminosity, and radius from ~ 1 –100 Myr provided by measurements of rotation, dynamical masses, and empirical isochrones on the H-R diagram.

4.2 Rotation

Much of the early work on the angular momentum evolution of young stars focused on rotational velocities measured from high-resolution spectra of absorption line profiles (Bouvier et al. 1986, Hartmann et al. 1986, Stauffer & Hartmann 1986). Because of the development of wide-field optical cameras in the 1990's, it became more efficient to trace angular momentum via rotation periods (in compact clusters), which can be measured from the photometric modulations caused by the rotation of spotted stellar surfaces. Rotation periods are now available for thousands of cluster members, including an increasing number of low-mass stars and brown dwarfs (Herbst et al. 2007).

For stars at ages of a few Myr, the largest studies of rotation periods have been conducted in the ONC and NGC 2264 ($\tau \sim 1$ and 2 Myr, Herbst, Bailer-Jones & Mundt 2001; Herbst et al. 2002; Lamm et al. 2005, 2004; Stassun et al. 1999). In any given mass range, stars in these clusters exhibit a broad distribution of periods, and hence angular momenta, covering a factor of 30 or more. The origin of a breadth of this kind at such young ages is unknown since rotation measurements at earlier, protostellar stages are difficult to obtain (Covey et al. 2005). For masses of 0.4 – $1.5 M_{\odot}$, the periods range from 0.6–20 days and have a bimodal distribution. Stars at lower masses rotate more rapidly on average and show a single peak in their period distribution. Although rotation periods are shorter at lower masses, the specific angular momentum remains roughly constant. These trends appear to continue into substellar masses, where young brown dwarfs rotate with periods of $\lesssim 1$ day (Cody & Hillenbrand 2010; Rodríguez-Ledesma, Mundt & Eislöffel 2009; Scholz & Eislöffel 2005). Scholz & Eislöffel (2005) suggested that some young low-mass objects rotate near 100% of the break-up period based on a small sample in ϵ Ori, but Cody & Hillenbrand (2010) found that the maximum rotation period is 40% of break-up in a larger sample in σ Ori. The fraction of low-mass stars and brown dwarfs that show periodic variability is lower than the fraction for solar-type stars, probably because of weaker magnetic fields and fewer spots (Cody & Hillenbrand 2010). In addition to measuring rotation periods, the

photometric monitoring of Cody & Hillenbrand (2010, 2011) found no evidence that young brown dwarfs undergo pulsations from the instabilities examined by Palla & Baraffe (2005).

To explain the presence of slowly rotating stars at ages of only a few Myr, it has been proposed that a young star can lose angular momentum by transferring it to a circumstellar disk via the stellar magnetic field (“disk locking”, Herbst et al. 2007, references therein). If this mechanism is valid, then slow rotators should show a higher frequency of disks. This prediction was tested initially with ground-based near-IR measurements of disk excesses, but mid-IR data from the *Spitzer Space Telescope* have enabled more conclusive tests, particularly for low-mass stars and brown dwarfs, whose disks often lack noticeable near-IR excesses. Among solar-type stars, slow rotators do show a higher frequency of disks, supporting the disk locking theory in this mass range (Cieza & Baliber 2007, Rebull et al. 2006). For low-mass stars, some studies have found evidence for a connection between rotation and disks (Rebull et al. 2006) while others have not (Cody & Hillenbrand 2010; Le Blanc, Covey & Stassun 2011). Thus, disk locking may be less efficient at lower stellar masses.

Rotation measurements have been compared among clusters across a wide range of ages to characterize the degree of angular momentum loss over time. Solar-type stars rotate progressively faster on average from the ONC to NGC 2264 to the zero age main sequence in the Pleiades, IC 2602, and α Per (Herbst & Mundt 2005). The specific angular momentum changes little over time for the faster rotators while stars that rotate slowly at ages of a few Myr seem to experience additional braking. Meanwhile, the evolution of low-mass stars is more closely described by conservation of angular momentum with only exponential wind braking (Scholz & Eislöffel 2004; Sills, Pinsonneault & Terndrup 2000; Terndrup et al. 2000). Few rotational data are available for brown dwarfs near ages of ~ 100 Myr for comparison to younger counterparts. Measurements for older brown dwarfs in the field indicate that they do eventually spin down, but on much longer timescales than stars (Blake, Charbonneau & Russel 2010; Irwin et al. 2011; Mohanty & Basri 2003; Reiners & Basri 2008; Scholz et al. 2011; Zapatero Osorio et al. 2006). This trend of decreasing angular momentum losses at lower masses has been attributed to changes in the mechanisms of magnetic field generation from solar-type stars to fully convective low-mass stars and brown dwarfs and the reduced coupling of atmospheres and magnetic fields at lower temperatures.

4.3 Dynamical Masses

The luminosity, temperature, and radius predicted by evolutionary models for a given mass and age can be tested by comparison to the observed properties of stars and brown dwarfs whose masses are known independently from dynamical measurements. Binary systems are the most common source of dynamical masses, but it also has been possible to estimate the masses of a few young stars via the rotational velocities of their circumstellar disks (Simon, Dutrey & Guilloteau 2000). Dynamical masses have been measured for a few dozen pre-main-sequence stars, and compilations of these data have been used to characterize the sizes of systematic errors in various sets of models and the possible sources of those errors (Baraffe et al. 2002, Hillenbrand & White 2004, Luhman et al. 2003b, Mathieu et al. 2007).

We now examine the model constraints provided by the small number of young low-mass stars and brown dwarfs for which dynamical data are available. These

objects consist of two eclipsing binaries in the ONC, JW 380 (0.15 and 0.26 M_{\odot} , Irwin et al. 2007) and 2MASS J05352184-0546085 (0.0366 and 0.0572 M_{\odot} , Gómez Maqueo Chew et al. 2009; Stassun, Mathieu & Valenti 2006), the spectroscopic binary PPl 15 ($q = 0.85$, Basri & Martín 1999), and the resolved companion AB Dor C (0.09 M_{\odot} , Close et al. 2005, Guirado et al. 2006). The measured radii of the components of JW 380 are consistent with the values predicted by most models for an age of a few Myr (Irwin et al. 2007). We have measured a spectral type of M4.5 from an optical spectrum of the system. When combined with the temperature scale from Luhman et al. (2003b) and the 1 Myr isochrone of Baraffe et al. (1998), this classification implies a mass of $\sim 0.2 M_{\odot}$, which falls between the dynamical masses of the components as it should. Thus, the data for JW 380 suggest that the IMFs for star-forming clusters that are based primarily on spectral types, like those in Figure 6, do not have large systematic errors near 0.2 M_{\odot} . JW 380 also confirms that the peak in the spectral type distributions for star-forming regions corresponds to a mass of $\sim 0.15 M_{\odot}$ (Figure 5).

Like JW 380, the radii of the components of 2MASS J05352184-0546085 (hereafter 2M 0535-0546) are in rough agreement with the predictions of evolutionary models (Stassun, Mathieu & Valenti 2006, 2007). A spectral type of M6.5 has been estimated for the primary (Stassun, Mathieu & Valenti 2006) while we classify a spectrum of the combined system as M6.75. Thus, this system has confirmed that newborn brown dwarfs are as large and warm as old low-mass stars. However, the eclipse data have shown that the primary is warmer than the secondary, which is contrary to the expectations of standard evolutionary models. It has been suggested that the primary may be unusually cool (and large) for its mass because of a strong surface magnetic field and/or a large spot coverage (Chabrier, Gallardo & Baraffe 2007; MacDonald & Mullan 2009; Stassun, Mathieu & Valenti 2007). The primary rotates faster than the secondary and exhibits stronger chromospheric H α emission (Reiners et al. 2007), which suggests that it is indeed magnetically active. Low-mass stars in tight eclipsing binaries in the field also tend to be cooler and larger than expected based on theoretical predictions (Morales et al. 2009, references therein). A magnetic origin for this anomaly is supported by recent studies indicating that the radii of stars in wider binaries are less inflated relative to the models (Coughlin et al. 2011, Kraus et al. 2011a) and that single rapid rotators and active stars may be cooler and larger than normal (Jackson, Jeffries & Maxted 2009; Morales, Ribas & Jordi 2008). If this explanation for the temperature reversal of 2M 0535-0546 is correct, then the spectral types of young brown dwarfs may be altered by the presence of activity, leading to errors in the mass estimates of individual objects (Mohanty, Stassun & Mathieu 2009). We discuss the implications of this source of error on measurements of the IMF in Section 4.5. Additional tests of the evolutionary models at young ages and low masses should soon be available via new eclipsing binaries that have been recently discovered in the ONC (Morales-Calderón et al. 2011, Morales-Calderón, in preparation).

Since the age of AB Dor is similar to that of the Pleiades ($\tau = 75\text{--}150$ Myr, Luhman, Stauffer & Mamajek 2005), it is useful to discuss AB Dor C and PPl 15 together. As with JW 380 and 2M 0535-0546, we can use AB Dor C and PPl 15 to help calibrate the relation between mass and spectral type, but now at an age of ~ 100 Myr. AB Dor C has been classified as M5.5–M6 (Close et al. 2007, Luhman & Potter 2006) and the components of PPl 15 likely have spectral types of M6 and M7 (Basri & Martín 1999). Since the dynamical measurements of

PPl 15 have provided only a mass ratio rather than individual masses, we instead make use of the upper mass limit of $0.1 M_{\odot}$ for each component derived from the presence of Li (Basri, Marcy & Graham 1996; Basri & Martín 1999). The mass constraints for AB Dor C and PPl 15 combined with their spectral types suggest that the hydrogen burning limit occurs near M6 at ages of ~ 100 Myr, which is consistent with the temperature predicted by evolutionary models (e.g., Chabrier et al. 2000b) for a reasonable choice of temperature scale (Luhman 1999). The near-IR absolute magnitudes of AB Dor C are also consistent with the values predicted for its age (Boccaletti et al. 2008).

Finally, we note that significant progress has been made over the last few years in measurements of dynamical masses for low-mass stars and brown dwarfs in the field (Dupuy et al. 2010, Konopacky et al. 2010). These data are valuable for testing models of older brown dwarfs ($\tau \gtrsim 0.5$ Gyr), but the results of those tests are not directly relevant to the early evolution of low-mass objects since the likely sources of error in the models differ between different regimes of temperature and age.

4.4 Hertzsprung-Russell Diagram

Empirical isochrones formed by the members of multiple systems and young clusters have long been used to assess the validity of theoretical isochrones. This test has been applied to young low-mass objects in star-forming regions down to spectral types of M9 (Kraus & Hillenbrand 2009b, Luhman 2004a, White et al. 1999), revealing relatively good agreement between the empirical isochrones and some sets of models (Baraffe et al. 1998), particularly when flexibility in the temperature scale is allowed (Luhman 1999, Luhman et al. 2003b, Section 2.5.2). In this section, we expand this work to later types and older ages by considering the best available samples of objects later than M6 and younger than $\lesssim 100$ Myr. By doing so, we hope to more fully illuminate the evolutionary paths taken by young, low-mass objects.

To display the early evolution of low-mass stars and brown dwarfs, we plot objects on a diagram of M_{K_s} versus spectral type. We use an H-R diagram in terms of observed properties rather than temperature and luminosity to preserve the data in their original form and to avoid the uncertainties associated with estimates of temperature and luminosity. Spectral type is the best observational proxy for temperature, and it can be measured quite precisely with the proper data and methods. Among the standard broad-band filters, we use M_{K_s} as a substitute for luminosity because, in this band, excess emission from disks around late-type objects is negligible and extinction is low. M_{K_s} should also be a better choice than bands at shorter wavelengths since the near-IR colors of young objects become unusually red at the latest types (Section 2.5.4).

For our H-R diagram, we have selected young populations in which the known members extend to spectral types of \gtrsim L0. This sample consists of Taurus ($\tau \sim 1$ Myr), Chamaeleon ($\tau \sim 2$ –3 Myr), TWA ($\tau \sim 10$ Myr), Upper Sco ($\tau \sim 12$ Myr), and the Pleiades ($\tau \sim 100$ –125 Myr, see Sections 2.3, 2.4). We also include young field dwarfs and young companions for which accurate spectral types and parallaxes are available. The former are from Faherty et al. (2012) and the latter consist of the previously discussed companions 2M 1207-3932 B, HR 8799 b, and HN Peg B, as well as AB Pic B (Bonnetfoy et al. 2010, Chauvin et al. 2005) and HD 203030 B (Metchev & Hillenbrand 2006). G 196-3 B is another compan-

ion that is cool, young, and well-studied (Zapatero Osorio et al. 2010), but it is excluded since it lacks a parallax measurement. Similarly, we consider only the members of TWA that have parallax data. The H-R diagram for these populations is shown in Figure 9. We have attempted to ensure that the adopted spectral types are on the same classification system, and have reclassified a few objects with spectra from the literature and our unpublished data. We have also omitted sources that appear to have uncertain spectral types or membership. Most of the photometry is from 2MASS and UKIDSS, and no correction has been made for known binaries that are unresolved in those images. For comparison, we include in Figure 9 a fit to the sequence of M, L, and T dwarfs in the field ($\tau > 1$ Gyr, Faherty et al. 2012).

In analyzing the cluster sequences, we begin by examining their thicknesses in M_{K_s} . The sequences for Taurus, Chamaeleon, and Upper Sco have widths of 1–2 mag in M_{K_s} at a given spectral type while the Pleiades sequence is much more narrow, and most of its bright outliers are known binaries. Large vertical spreads are universally seen at higher mass as well for star-forming regions, and have been primarily attributed to either a wide distribution of ages or observational uncertainties (Hartmann 2001, Palla & Stahler 2002). The latter should be minimized in our H-R diagram since the photometry is fairly accurate in most cases, extinction errors are small in the K_s band, many of the spectral types have been measured in the same manner, disk emission is negligible, and there is little if any contamination from non-members. Unresolved binaries can introduce a spread of 0.75 mag and the large diameters of Taurus and Upper Sco correspond to a range of ~ 0.35 mag in the distance moduli of their members. The sequences seem somewhat thicker than expected from these effects alone, so it is possible that a significant spread of M_{K_s} is truly present. If so, it may reflect a spread in radii rather than ages. For instance, the ONC appears to exhibit a wide distribution of radii that is not attributable to ages (Jeffries 2007, Jeffries et al. 2011), and instead may be caused by differences in accretion histories (Baraffe, Chabrier & Gallardo 2009; Littlefair et al. 2011), although this interpretation has been challenged (Hosokawa, Offner & Krumholz 2011). The observation that members of binaries in Taurus are more coeval on the H-R diagram than random pairs of Taurus members suggests that at least a small portion of the luminosity spread in this region is due to a range of ages (Kraus & Hillenbrand 2009b, White & Ghez 2001).

The comparison of cluster sequences in Figure 9 provides a test of some of the basic predictions for the early evolution of low-mass objects. For instance, theoretical isochrones and mass tracks converge into one narrow sequence below ~ 1500 K since at these temperatures all brown dwarfs are predicted to have similar radii, even the younger ones (Baraffe et al. 1998, Burrows et al. 1997, Chabrier et al. 2000b). Indeed, this feature is evident in Figure 9, where the cluster sequences steadily converge from earlier to later spectral types, eventually approaching the sequence for field dwarfs. Although the temperature scale for young brown dwarfs is uncertain, particularly at later types (see below), it is useful to attempt a quantitative comparison to the predicted luminosity evolution. From Taurus to the Pleiades, the median sequences fade by ~ 3.5 and 1 mag in M_{K_s} at M7 and L0, respectively, which is consistent with the predicted changes in luminosity from 1–100 Myr for 2900 and 2200 K.

The behavior of the coolest objects in Figure 9 is quite peculiar. With the exception of the members of star-forming regions, young sources later than M9

fall on or below the sequence for field dwarfs, which is unexpected since young brown dwarfs should always be brighter than older ones at a given temperature. A number of studies have separately stumbled across the underluminous nature of objects in Figure 9. Based on their unusually red colors (Section 2.5.4) and their temperatures estimated from model spectra, 2M 1207-3932 B and the companions to HR 8799 appear below theoretical isochrones for their expected ages (Bowler et al. 2010, Mohanty et al. 2007). HD 203030 B and HN Peg B have been reported to be cooler than field dwarfs with the same spectral types (Luhman et al. 2007a, Metchev & Hillenbrand 2006), which is equivalent to saying that, if they have the same temperature as field dwarfs with the same types, then they are too faint for their youth (i.e., underluminous). The presence of this common anomaly has been recognized for subsets of these objects (Bowler et al. 2010; Currie et al. 2011; Metchev, Marois & Zuckerman 2009; Skemer et al. 2011). Metchev, Marois & Zuckerman (2009) and Bowler et al. (2010) attributed it to a gravity dependence of the temperature of the L/T transition, but Figure 9 shows that earlier L dwarfs appear underluminous as well. Meanwhile, Currie et al. (2011) suggested that the origin of this property is related to the planetary nature of the companions. Through their work on young field dwarfs, Faherty et al. (2012) realized that these young companions and young L dwarfs are both unusually red in near-IR bands and appear to be underluminous, concluding that their youth is the source of these characteristics. We now add to the objects that follow this pattern by noting that the sequences for young clusters like Taurus and Chamaeleon become underluminous relative to theoretical isochrones for spectral types later than M9 (Luhman et al. 2009b, Luhman & Muench 2008).

The underluminous positions of young objects in Figure 9 and other varieties of H-R diagrams can be partially explained by the fact that the near- to mid-IR colors of young objects later than M9 are redder than those of their field counterparts, and thus do not have the same bolometric corrections (Section 2.5.4). It is also likely that the temperature scale for young L and T dwarfs is significantly cooler than that of field dwarfs. The latter explanation is supported by the work of Barman et al. (2011a,b), who were able to successfully fit the SEDs of HR 8799 b and 2M 1207-3932 B with models of low-gravity, cloudy atmospheres that experience non-equilibrium chemistry. According to their models, a much lower temperature is needed for methane absorption to appear in young objects than in field dwarfs. As a result, Barman et al. (2011b) suggested that only extremely low-mass members of star-forming regions should be cool enough to exhibit methane and appear as T dwarfs.

Although the data in Figure 9 reveal a systematic pattern in the photometric properties of young L dwarfs, we point out one anomalous aspect. All of the young L dwarfs from the field have gravity-sensitive lines that are indicative of ages of $\lesssim 100$ Myr, so it is unclear why two of the L0 dwarfs appear well below the Pleiades sequence. In fact, one of these objects, 2MASS J00325584-4405058, has been classified as L0 δ , which suggests an age of ~ 10 Myr (Cruz, Kirkpatrick & Burgasser 2009). A similar, yet smaller, discrepancy is present for AB Pic B, which is believed to have an age of 30 Myr but is slightly fainter than its counterpart in the Pleiades. It would be interesting to directly compare spectra of the various objects near L0 to verify that they have the same spectral types, determine their relative surface gravities, and assess whether the latter are consistent with their relative absolute magnitudes.

4.5 Accuracy of IMF Measurements in Young Clusters

Given the possible errors in evolutionary models described in the previous sections, it is useful to discuss the resulting implications for IMF estimates in young clusters. Since very few cluster members have been spectroscopically confirmed at types later than M9, the errors in bolometric corrections and temperature scales described earlier for young L dwarfs have little impact on previous IMF measurements. For the IMFs in the youngest clusters (e.g, Figure 6), the masses are derived from positions in the H-R diagram, and hence depend very little on luminosity. As a result, processes that primarily affect luminosity, such as episodic accretion, should not introduce large errors into the mass estimates. On the other hand, the spectral types of young low-mass stars and brown dwarfs may be altered by magnetic activity (Section 4.3). To gauge the magnitude of this source of error, we can consider the width of the peak in the distribution of spectral types for a star-forming region. As shown in Figure 5, peaks for both IC 348 and Chamaeleon I are rather narrow, which indicates that most of the low-mass members are not experiencing large variations in spectral type (> 1 subclass). If that was the case, then the spectral type peak would be much broader, and the abrupt decline later than M5 would not be present. Furthermore, the possible presence of activity-induced errors in spectral types does not fundamentally change the outlook for the IMF's accuracy since comparable errors are likely already present. For instance, for a typical member of a star-forming region, the published spectral types often differ by a few subclasses, and these classification errors can be either random or systematic (the members of IC 348 and Chamaeleon I in Figure 5 have been classified in an unusually uniform manner). Derivations of IMFs for young clusters are subject to various other sources of error, such as the choice of temperature scale and the evolutionary models. However, all measurements of the IMF, regardless of the type of stellar population, are subject to random and systematic errors, many of which are often difficult to quantify. The relevant question is not whether such errors exist, but whether the final IMF produced by a given methodology is accurate. The random errors for masses in young clusters will simply smooth out any small-scale structure in the IMF, and thus are unimportant for the measurements of broad features and slopes, particularly given the large sizes of the mass bins that are generally used. Meanwhile, systematic errors in mass estimates will stretch or contract the IMF, perhaps to a different degree as a function of mass. The agreement between the IMFs of star-forming regions, open clusters, and the field indicates that large errors of this kind are not present at masses higher than $\sim 0.02 M_{\odot}$ (Figure 6, Luhman & Potter 2006). However, IMF estimates in young clusters are untested at lower masses, and could have significant errors given the peculiar photometric properties of young L and T dwarfs and the resulting uncertainties in their temperatures and luminosities.

5 Concluding Remarks

The absence of a significant dependence of the abundance of brown dwarfs on stellar density or the presence of O stars, the ability of brown dwarfs to form in isolation and in wide binaries, and the likely existence of protostellar brown dwarfs together provide compelling evidence that brown dwarfs can form without the involvement of tidal shear in massive cluster-forming cores, dynamical

interactions, disk fragmentation around solar-type stars, or photoionizing radiation. Thus, it seems likely that the one remaining formation mechanism from Section 3.1, turbulent fragmentation, is responsible for some fraction of brown dwarfs, and perhaps most of the ones in low-density regions like Taurus. It is possible that other proposed mechanisms also produce brown dwarfs, particularly in dense clusters, although there is not any clear observational evidence of this so far. One of the most promising avenues for better understanding the formation of brown dwarfs is continued study of low-mass protostars by identifying them in larger numbers with data from *Spitzer*, WISE, and *Herschel Observatory* and by detailed followup observations with facilities like the Atacama Large Millimeter Array.

Measurements of dynamical masses for a small number of young low-mass stars and brown dwarfs have confirmed the theoretical prediction that the hydrogen burning mass limit occurs near a spectral type of M6 for ages of ~ 1 –100 Myr. Based on a wide variety of studies, young objects later than \sim M9, including planetary-mass companions, exhibit unusually red colors and faint absolute magnitudes at near-IR wavelengths relative to older field dwarfs. It appears that this behavior can be explained with model atmospheres that have clouds, low gravities, and non-equilibrium chemistry. Further testing and refinement of the atmospheric and evolutionary models at young ages and low masses will require additional measurements of dynamical masses and larger samples of well-characterized young L and T dwarfs.

ACKNOWLEDGMENTS

We thank John Bochanski, Jacqueline Faherty, Eric Feigelson, Lee Hartmann, William Herbst, Adam Kraus, Dagny Looper, Eric Mamajek, and John Stauffer for access to unpublished results and comments on the manuscript. We acknowledge support from grant AST-0544588 from the National Science Foundation. The Center for Exoplanets and Habitable Worlds is supported by the Pennsylvania State University, the Eberly College of Science, and the Pennsylvania Space Grant Consortium.

References

1. Adame L, et al. 2011. *Astrophys. J.* 726:L3
2. Allard F, Hauschildt PH, Alexander DR, Starrfield S. 1997. *Ann. Rev. Astron. Astrophys.* 35:137
3. Allen PR, Koerner DW, Reid IN. 2005 *Astrophys. J.* 625:385
4. Allers KN, Liu MC, Dupuy TJ, Cushing MC. 2010. *Astrophys. J.* 715:561
5. Allers KN, et al. 2007. *Astrophys. J.* 657:511
6. Alves de Oliveira C, et al. 2010. *Astron. & Astrophys.* 515:A75
7. Andersen M, et al. 2006. *Astron. J.* 132:2296
8. André P, Ward-Thompson D, Barsony M. 1993. *Astrophys. J.* 406:122
9. André P, et al. 2010. *Astron. & Astrophys.* 518:L102
10. Andrews SM, Liu MC, Williams JP, Allers KN. 2008. *Astrophys. J.* 685:1039
11. Apai D, et al. 2004. *Astron. & Astrophys.* 426:L53

12. Apai D, et al. 2005. *Science* 310:834
13. Bannister NP, Jameson RF. 2007. *MNRAS* 378:L24
14. Baraffe I, Chabrier G, Allard F, Hauschildt PH. 1998. *Astron. & Astrophys.* 337:403
15. Baraffe I, Chabrier G, Allard F, Hauschildt PH. 2002. *Astron. & Astrophys.* 382:563
16. Baraffe I, Chabrier G, Gallardo J. 2009. *Astrophys. J.* 702:L27
17. Barman TS, Macintosh B, Konopacky QM, Marois C. 2011a. *Astrophys. J.* 733:65
18. Barman TS, Macintosh B, Konopacky QM, Marois C. 2011b. *Astrophys. J.* 735:L39
19. Barrado y Navascués D, Stauffer JR, Jayawardhana R. 2004. *Astrophys. J.* 614:386
20. Barrado y Navascués D, et al. 2004. *Astrophys. J.* 610:1064
21. Basri G. 2000. *Ann. Rev. Astron. Astrophys.* 38:485
22. Basri G, Marcy GW, Graham JR. 1996. *Astrophys. J.* 458:600
23. Basri G, Martín EL. 1999. *Astron. J.* 118:2460
24. Basri G, Reiners A. 2006. *Astron. J.* 132:663
25. Bastian N, Covey KR, Meyer MR. 2010. *Ann. Rev. Astron. Astrophys.* 48:339
26. Bate MR. 2009. *MNRAS* 392:590
27. Bate MR. 2012. *MNRAS* 419:3115
28. Bate MR, Bonnell IA. 2005. *MNRAS* 356:1201
29. Bate MR, Bonnell IA, Bromm V. 2002. *MNRAS* 332:L65
30. Bate MR, Bonnell IA, Bromm V. 2003. *MNRAS* 339:577
31. Becklin EE, Zuckerman B. 1988. *Nature* 336:656
32. Béjar VJS, Zapatero Osorio MR, Rebolo R. 1999. *Astrophys. J.* 521:671
33. Béjar VJS, et al. 2001. *Astrophys. J.* 556:830
34. Bergfors C, et al. 2010. *Astron. & Astrophys.* 520:A54
35. Bihain G, et al. 2006. *Astron. & Astrophys.* 458:805
36. Bihain G, et al. 2010. *Astron. & Astrophys.* 519:A93
37. Biller B, et al. 2011. *Astrophys. J.* 730:39
38. Blake CH, Charbonneau D, Russel JW. 2010. *Astrophys. J.* 723:684
39. Boccaletti A, Chauvin G, Baudoz P, Beuzit J-L. 2008. *Astron. & Astrophys.* 482:939
40. Bochanski JJ, et al. 2010. *Astron. J.* 139:2679
41. Bonnefoy M, et al. 2010. *Astron. & Astrophys.* 512:A52
42. Bonnell IA, Clark P, Bate MR. 2008. *MNRAS* 389:1556
43. Bonnell IA, Larson RB, Zinnecker H. 2007. In *Protostars and Planets V*. ed. B Reipurth, D Jewitt, K Keil, Tucson:University of Arizona Press 149
44. Bonnell IA, Smith RJ, Clark PC, Bate MR. 2011. *MNRAS* 410:2339
45. Boss A. 1988. *Astrophys. J.* 331:370

46. Boss A. 2001. *Astrophys. J.* 551:L167
47. Bourke TL, et al. 2005. *Astrophys. J.* 633:L129
48. Bourke TL, et al. 2006. *Astrophys. J.* 649:L37
49. Bouvier J, Bertout C, Benz W, Mayor M. 1986. *Astron. & Astrophys.* 165:110
50. Bouvier J, et al. 2008. *Astron. & Astrophys.* 481:661
51. Bouy H, et al. 2003. *Astron. J.* 126:1526
52. Bowler BP, Liu MC, Dupuy TJ, Cushing MC. 2010. *Astrophys. J.* 723:850
53. Boyd DFA, Whitworth AP. 2005. *Astron. & Astrophys.* 430:1059
54. Briceño C, et al. 2002. *Astrophys. J.* 580:317
55. Burgasser AJ. 2004. *Astrophys. J. Suppl.* 155:191
56. Burgasser AJ, et al. 2003. *Astrophys. J.* 586:512
57. Burgasser AJ, et al. 2004. *Astrophys. J.* 604:827
58. Burgasser AJ, et al. 2006. *Astrophys. J.* 637:1067
59. Burgasser AJ, et al. 2007. In *Protostars and Planets V.* ed. B Reipurth, D Jewitt, K Keil, Tucson:University of Arizona Press 427
60. Burgess ASM, et al. 2009. *Astron. & Astrophys.* 508:823
61. Burningham B, et al. 2010. *MNRAS* 406:1885
62. Burrows A, et al. 1997. *Astrophys. J.* 491:856
63. Carpenter JM, Mamajek EE, Hillenbrand LA, Meyer MR. 2006. *Astrophys. J.* 651:L49
64. Casewell SL, et al. 2007. *MNRAS* 378:1131
65. Casewell SL, et al. 2011. *MNRAS* 412:2071
66. Chabrier G. 2001. *Astrophys. J.* 554:1274
67. Chabrier G. 2002. *Astrophys. J.* 567:304
68. Chabrier G, Baraffe I. 2000. *Ann. Rev. Astron. Astrophys.* 38:337
69. Chabrier G, Baraffe I, Allard F, Hauschildt P. 2000a. *Astrophys. J.* 542:L119
70. Chabrier G, Baraffe I, Allard F, Hauschildt P. 2000b. *Astrophys. J.* 542:464
71. Chabrier G, Gallardo J, Baraffe I. 2007. *Astron. & Astrophys.* 427:L17
72. Chabrier G, Hennebelle P. 2010. *Astrophys. J.* 725:L79
73. Chabrier G, et al. 2007. In *Protostars and Planets V.* ed. B Reipurth, D Jewitt, K Keil, Tucson:University of Arizona Press 623
74. Chauvin G, et al. 2004. *Astron. & Astrophys.* 425:L29
75. Chauvin G, et al. 2005. *Astron. & Astrophys.* 438:L29
76. Cieza L, Baliber N. 2007. *Astrophys. J.* 671:605
77. Clarke CJ, Pringle JE. 2006. *MNRAS* 370:L10
78. Clarke JRA, et al. 2010. *MNRAS* 402:575
79. Close LM, Siegler N, Freed M, Biller B. 2003. *Astrophys. J.* 587:407
80. Close LM, et al. 2005. *Nature* 433:286
81. Close LM, et al. 2007. *Astrophys. J.* 665:736

82. Cody AM, Hillenbrand LA. 2010. *Astrophys. J. Suppl.* 191:389
83. Cody AM, Hillenbrand LA. 2011. *Astrophys. J.* 741:9
84. Comerón F, Rieke GH, Burrows A, Rieke MJ. 1993. *Astrophys. J.* 416:185
85. Comerón F, Rieke GH, Neuhäuser R. 1999. *Astron. & Astrophys.* 343:477
86. Comerón F, et al. 1998. *Astron. & Astrophys.* 335:522
87. Coughlin JL, et al. 2011. *Astron. J.* 141:78
88. Covey KR, Greene TP, Doppmann GW, Lada CJ. 2005. *Astron. J.* 129:2765
89. Covey KR, et al. 2008. *Astron. J.* 136:1778
90. Cruz KL, Kirkpatrick JD, Burgasser AJ. 2009. *Astron. J.* 137:3345
91. Cruz KL, et al. 2007. *Astron. J.* 133:439
92. Currie T, et al. 2011. *Astrophys. J.* 729:128
93. Cushing MC, et al. 2011. *Astrophys. J.* 743:50
94. Deacon NR, Nelemans G, Hambly NC. 2008. *Astron. & Astrophys.* 486:283
95. Dunham MM, et al. 2006. *Astrophys. J.* 651:945
96. Dunham MM, et al. 2008. *Astrophys. J. Suppl.* 179:249
97. Dunham MM, et al. 2010. *Astrophys. J.* 721:995
98. Dupuy TJ, Liu MC. 2011. *Astrophys. J.* 733:122
99. Dupuy TJ, et al. 2010. *Astrophys. J.* 721:1725
100. Duquennoy A, Mayor M. 1991. *Astron. & Astrophys.* 248:485
101. Elmegreen BG. 2011. *Astrophys. J.* 731:61
102. Epchtein N, et al. 1999. *Astron. & Astrophys.* 349:236
103. Faherty JK, et al. 2009. *Astron. J.* 137:1
104. Faherty JK, et al. 2011. *Astron. J.* 141:71
105. Faherty JK, et al. 2012. *Astrophys. J.* in press
106. Feigelson ED, Lawson WA. 2004. *Astrophys. J.* 614:267
107. Feigelson ED, Lawson WA, Garmire GP. 2003. *Astrophys. J.* 599:1207
108. Fernández M, Comerón F. 2001 *Astron. & Astrophys.* 380:264
109. Finkbeiner DP, et al. 2004. *Astron. J.* 128:2577
110. Fischer DA, Marcy GW. 1992. *Astrophys. J.* 396:178
111. Furlan E, et al. 2005. *Astrophys. J.* 621:L129
112. Furlan E, et al. 2008. *Astrophys. J. Suppl.* 176:184
113. Furlan E, et al. 2011. *Astrophys. J. Suppl.* 195:3
114. Gálvez-Ortiz MC, et al. 2010. *MNRAS* 409:552
115. Gizis JE. 2002. *Astrophys. J.* 575:484
116. Golimowski DA, et al. 2004. *Astron. J.* 127:3516
117. Gómez Maqueo Chew Y, Stassun KG, Prša A, Mathieu RD. 2009. *Astrophys. J.* 699:1196
118. Goodwin SP, Whitworth A. 2007. *Astron. & Astrophys.* 466:943

119. Goodwin SP, Whitworth AP, Ward-Thompson D. 2004. *Astron. & Astrophys.* 419:543
120. Gorlova NI, Meyer MR, Rieke GH, Liebert J. 2003. *Astrophys. J.* 593:1074
121. Greene TP, Young ET. 1992. *Astrophys. J.* 395:516
122. Guieu S, et al. 2006. *Astron. & Astrophys.* 446:485
123. Guirado JC, et al. 2006. *Astron. & Astrophys.* 446:733
124. Haisch KE, Barsony M, Tinney C. 2010. *Astrophys. J.* 719:L90
125. Hambly NC, Hawkins MRS, Jameson RF. 1993. *Astro. Astrophys. Suppl. Ser.* 100:607
126. Hartmann L. 2001. *Astron. J.* 121:1030
127. Hartmann L, Cassen P, Kenyon SJ. 1997. *Astrophys. J.* 475:770
128. Hartmann L, D'Alessio P, Calvet N, Muzerolle J. 2006. *Astrophys. J.* 648:484
129. Hartmann L, Hewett R, Stahler S, Mathieu RD. 1986. *Astrophys. J.* 309:275
130. Hartmann L, et al. 1999. *Astron. J.* 118:1784
131. Harvey PM, et al. 2011. *Astrophys. J.* 744:L1
132. Hayashi C, Nakano T. 1963. *Prog. Theor. Phys.* 30:460
133. Hennebelle P, Chabrier G. 2008. *Astrophys. J.* 684:395
134. Henry TJ, Kirkpatrick JD, Simons DA. 1994. *Astron. J.* 108:1437
135. Herbst W, Bailer-Jones CAL, Mundt R. 2001. *Astrophys. J.* 554:L197
136. Herbst W, Mundt R. 2005. *Astrophys. J.* 633:967
137. Herbst W, et al. 2002. *Astron. & Astrophys.* 396:513
138. Herbst W, Eisloffel J, Mundt R, Scholz A. 2007. In *Protostars and Planets V*. ed. B Reipurth, D Jewitt, K Keil, Tucson:University of Arizona Press 297
139. Herczeg GJ, Hillenbrand LA. 2008. *Astrophys. J.* 681:594
140. Hester JJ, et al. 1996. *Astron. J.* 111:2349
141. Hillenbrand LA. 1997. *Astron. J.* 113:1733
142. Hillenbrand LA, Carpenter JM. 2000. *Astrophys. J.* 540:236
143. Hillenbrand LA, White RJ. 2004. *Astrophys. J.* 604:741
144. Hosokawa T, Offner SSR, Krumholz MR. 2011. *Astrophys. J.* 738:140
145. Irwin J, et al. 2007. *MNRAS* 380:541
146. Irwin J, et al. 2011. *Astrophys. J.* 727:56
147. Jackson RJ, Jeffries RD, Maxted PFL. 2009. *MNRAS* 399:L89
148. Jameson RF, Skillen I. 1989. *MNRAS* 239:247
149. Jayawardhana R, Ardila DR, Stelzer B, Haisch KE. 2003. *Astron. J.* 126:1515
150. Jayawardhana R, Mohanty S, Basri G. 2002. *Astrophys. J.* 578:L141
151. Jeffries RD. 2007. *MNRAS* 381:1169
152. Jeffries RD, Littlefair SP, Naylor T, Mayne NJ. 2011. *MNRAS* 418:1948
153. Joergens V. 2006. *Astron. & Astrophys.* 448:655
154. Joergens V, Guenther E. 2001. *Astron. & Astrophys.* 379:L9

155. Kauffmann J, et al. 2011. *MNRAS* 416:2341
156. Kenyon SJ, Hartmann L. 1995. *Astrophys. J. Suppl.* 101:117
157. Kessler-Silacci JE, et al. 2007. *Astrophys. J.* 659:680
158. Kirkpatrick JD. 2005. *Ann. Rev. Astron. Astrophys.* 43:195
159. Kirkpatrick JD, Henry TJ, Irwin MJ. 1997. *Astron. J.* 113:1421
160. Kirkpatrick JD, Henry TJ, Liebert J. 1993. *Astrophys. J.* 406:701
161. Kirkpatrick JD, Henry TJ, McCarthy DW. 1991. *Astrophys. J. Suppl.* 77:417
162. Kirkpatrick JD, et al. 1999a. *Astrophys. J.* 519:802
163. Kirkpatrick JD, et al. 1999b. *Astrophys. J.* 519:834
164. Kirkpatrick JD, et al. 2006. *Astrophys. J.* 639:1120
165. Kirkpatrick JD, et al. 2008. *Astrophys. J.* 689:1295
166. Kirkpatrick JD, et al. 2011. *Astrophys. J. Suppl.* 197:19
167. Klein R, et al. 2003. *Astrophys. J.* 593:L57
168. Konopacky QM, Ghez AM, Rice EL, Duchêne G. 2007. *Astrophys. J.* 663:394
169. Konopacky QM, et al. 2010. *Astrophys. J.* 711:1087
170. Kraus AL, Hillenbrand LA. 2007. *Astrophys. J.* 662:413
171. Kraus AL, Hillenbrand LA. 2009a. *Astrophys. J.* 703:1511
172. Kraus AL, Hillenbrand LA. 2009b. *Astrophys. J.* 704:531
173. Kraus AL, Hillenbrand LA. 2012. *Astrophys. J.* submitted
174. Kraus AL, Ireland MJ, Martinache F, Hillenbrand LA. 2011b. *Astrophys. J.* 731:8
175. Kraus AL, White RJ, Hillenbrand LA. 2005. *Astrophys. J.* 633:452
176. Kraus AL, White RJ, Hillenbrand LA. 2006. *Astrophys. J.* 649:306
177. Kraus AL, et al. 2011a. *Astrophys. J.* 728:48
178. Kroupa P. 2002. *Science* 295:82
179. Kroupa P, Bouvier J. 2003. *MNRAS* 346:369
180. Kumar SS. 1963. *Astrophys. J.* 137:1121
181. Kurosawa R, Harries TJ, Littlefair SP. 2006. *MNRAS* 372:1879
182. Lada CJ. 1987. in IAU Symp. 115, Star Forming Regions, ed. M. Peimbert & J. Jugaku (Dordrecht: Reidel) 1
183. Lada CJ, Lada EA. 2003. *Ann. Rev. Astron. Astrophys.* 41:57
184. Lada CJ, et al. 2006. *Astron. J.* 131:1574
185. Lada CJ, et al. 2008. *Astrophys. J.* 672:410
186. Lada EA, Lada CJ. 1995. *Astron. J.* 109:1682
187. Lafrenière D, et al. 2008. *Astrophys. J.* 683:844
188. Lamm MH, Mundt R, Bailer-Jones CAL, Herbst W. 2005. *Astron. & Astrophys.* 430:1005
189. Lamm MH, et al. 2004. *Astron. & Astrophys.* 417:557
190. Latham DW, et al. 1989. *Nature* 339:38
191. Lawrence A, et al. 2007. *MNRAS* 379:1599

192. Lawson WA, Crause LA, Mamajek EE, Feigelson ED. 2002. *MNRAS* 329:L29
193. Le Blanc TS, Covey KR, Stassun KG. 2011. *Astron. J.* 142:55
194. Lee CW, et al. 2009. *Astrophys. J.* 693:1290
195. Littlefair SP, et al. 2011. *MNRAS* 413:L56
196. Liu MC, Najita J, Tokunaga AT. 2003. *Astrophys. J.* 585:372
197. Lodieu N, Dobbie PD, Hambly NC. 2011 *Astron. & Astrophys.* 527:A24
198. Lodieu N, Hambly NC, Jameson RF. 2006. *MNRAS* 373:95
199. Lodieu N, Hambly NC, Jameson RF, Hodgkin ST. 2008. *MNRAS* 383:1385
200. Lodieu N, et al. 2005. *Astron. & Astrophys.* 436:853
201. Looper DL, Burgasser AJ, Kirkpatrick JD, Swift BJ. 2007. *Astrophys. J.* 669:L97
202. Looper DL, et al. 2010. *Astrophys. J.* 714:45
203. Low C, Lynden-Bell D. 1976. *MNRAS* 176:367
204. Lucas PW, Roche PF. 2000. *MNRAS* 314:858
205. Lucas PW, Roche PF, Allard F, Hauschildt PH. 2001. *MNRAS* 326:695
206. Lucas PW, Roche PF, Tamura M. 2005. *MNRAS* 361:211
207. Luhman KL. 1999. *Astrophys. J.* 525:466
208. Luhman KL. 2000. *Astrophys. J.* 544:1044
209. Luhman KL. 2004a. *Astrophys. J.* 614:398
210. Luhman KL. 2004b. *Astrophys. J.* 616:1033
211. Luhman KL. 2004c. *Astrophys. J.* 617:1216
212. Luhman KL. 2006. *Astrophys. J.* 645:676
213. Luhman KL. 2007. *Astrophys. J. Suppl.* 173:104
214. Luhman KL. 2008. in Handbook of Star Forming Regions, Vol. II, The Southern Sky, ed. B. Reipurth (ASP Monograph Publ. Vol. 5; San Francisco, CA: ASP), 169
215. Luhman KL, Briceño C, Rieke GH, Hartmann L. 1998. *Astrophys. J.* 493:909
216. Luhman KL, Liebert J, Rieke GH. 1997. *Astrophys. J.* 489:L165
217. Luhman KL, Mamajek EE. 2010. *Astrophys. J.* 716:L120
218. Luhman KL, Mamajek EE, Cruz KL, Allen, PR. 2009b. *Astrophys. J.* 703:399
219. Luhman KL, Muench AA. 2008. *Astrophys. J.* 684:654
220. Luhman KL, Potter D. 2006. *Astrophys. J.* 638:887
221. Luhman KL, Stauffer JR, Mamajek EE. 2005. *Astrophys. J.* 628:L69
222. Luhman KL, Steeghs D. 2004. *Astrophys. J.* 609:917
223. Luhman KL, et al. 2000. *Astrophys. J.* 540:1016
224. Luhman KL, et al. 2003a. *Astrophys. J.* 590:348
225. Luhman KL, et al. 2003b. *Astrophys. J.* 593:1093
226. Luhman KL, et al. 2005a. *Astrophys. J.* 631:L69
227. Luhman KL, et al. 2005b. *Astrophys. J.* 635:L93
228. Luhman KL, et al. 2006. *Astrophys. J.* 647:1180

229. Luhman KL, et al. 2007a. *Astrophys. J.* 654:570
230. Luhman KL, et al. 2007b. *Astrophys. J.* 659:1629
231. Luhman KL, et al. 2007c. *Astrophys. J.* 666:1219
232. Luhman KL, et al. 2007d. In *Protostars and Planets V.* ed. B Reipurth, D Jewitt, K Keil, Tucson:University of Arizona Press 443
233. Luhman KL, et al. 2008. *Astrophys. J.* 675:1375
234. Luhman KL, et al. 2009a. *Astrophys. J.* 691:1265
235. Luhman KL, et al. 2010. *Astrophys. J. Suppl.* 186:111
236. Lyo A-R, Lawson WA, Feigelson ED, Crause LA. 2004. *MNRAS* 347:246
237. MacDonald J, Mullan DJ. 2009. *Astrophys. J.* 700:387
238. Mamajek E, Lawson WA, Feigelson ED. 1999. *Astrophys. J.* 516:77
239. Marois C, et al. 2008. *Science* 322:1348
240. Marsh KA, Kirkpatrick JD, Plavchan P. 2010. *Astrophys. J.* 709:L158
241. Mathieu RD, et al. 2007. In *Protostars and Planets V.* ed. B Reipurth, D Jewitt, K Keil, Tucson:University of Arizona Press 411
242. Martin DC, et al. 2005. *Astrophys. J.* 619:L1
243. Martín EL, Rebolo R, Zapatero Osorio MR. 1996. *Astrophys. J.* 469:706
244. Martín EL, et al. 1998. *Astrophys. J.* 507:L41
245. Maxted PFL, Jeffries RD. 2005. *MNRAS* 362:L45
246. McCaughrean MJ, Stauffer JR. 1994. *Astron. J.* 108:1382
247. McGovern MR, et al. 2004. *Astrophys. J.* 600:1020
248. Metchev S, Hillenbrand L. 2006. *Astrophys. J.* 651:1166
249. Metchev S, Kirkpatrick JD, Berriman GB,Looper D. 2008. *Astrophys. J.* 676:1281
250. Metchev S, Marois C, Zuckerman B. 2009. *Astrophys. J.* 705:L204
251. Michel M, Kirk H, Myers PC. 2011. *Astrophys. J.* 735:51
252. Mohanty S, Basri G. 2003. *Astrophys. J.* 583:451
253. Mohanty S, Jayawardhana R, Barrado y Navascués D. 2003. *Astrophys. J.* 593:L109
254. Mohanty S, Jayawardhana R, Basri G. 2004. *Astrophys. J.* 609:885
255. Mohanty S, Jayawardhana R, Basri G. 2005. *Astrophys. J.* 626:498
256. Mohanty S, Jayawardhana R, Huélamo N, Mamajek E. 2007. *Astrophys. J.* 657:1064
257. Mohanty S, Stassun KG, Mathieu RD. 2009. *Astrophys. J.* 697:713
258. Mohanty S, et al. 2004a. *Astrophys. J.* 609:L33
259. Mohanty S, et al. 2004b. *Astrophys. J.* 609:854
260. Mohanty S, et al. 2012. *Astrophys. J.* submitted
261. Morales-Calderón M, et al. 2011. *Astrophys. J.* 733:50
262. Morales JC, Ribas I, Jordi C. 2008. *Astron. & Astrophys.* 478:507
263. Morales JC, et al. 2009. *Astrophys. J.* 691:1400

264. Moraux E, Bouvier J, Stauffer JR, Cuillandre J-C. 2003. *Astron. & Astrophys.* 400:891
265. Moraux E, Clarke C. 2005. *Astron. & Astrophys.* 429:895
266. Moraux E, Kroupa P, Bouvier J. 2004. *Astron. & Astrophys.* 426:75
267. Morrow AL, et al. 2008. *Astrophys. J.* 676:L143
268. Muench AA, Alves J, Lada CJ, Lada EA. 2001. *Astrophys. J.* 558:L51
269. Muench AA, Lada EA, Lada CJ, Alves J. 2002. *Astrophys. J.* 573:366
270. Muench AA, et al. 2003. *Astron. J.* 125:2029
271. Muench AA, et al. 2007. *Astron. J.* 134:411
272. Murphy SJ, Lawson WA, Bessell MS. 2010. *MNRAS* 406:L50
273. Muzerolle J, et al. 2000. *Astrophys. J.* 545:L141
274. Muzerolle J, et al. 2005. *Astrophys. J.* 625:906
275. Muzerolle J, et al. 2006. *Astrophys. J.* 643:1003
276. Muzerolle J, et al. 2010. *Astrophys. J.* 708:1107
277. Nakajima T, Tsuji T, Yanagisawa K. 2004. *Astrophys. J.* 607:499
278. Nakajima T, et al. 1995. *Nature* 378:463
279. Natta A, Testi L. 2001. *Astron. & Astrophys.* 376:L22
280. Natta A, Testi L, Randich S. 2006. *Astron. & Astrophys.* 452:245
281. Natta A, et al. 2002. *Astron. & Astrophys.* 393:597
282. Natta A, et al. 2004. *Astron. & Astrophys.* 424:603
283. Neuhäuser R, et al. 2002. *Astron. & Astrophys.* 384:999
284. Offner SSR, Klein RI, McKee CF. 2008. *Astrophys. J.* 686:1174
285. Offner SSR, Klein RI, McKee CF, Krumholz MR. 2009. *Astrophys. J.* 703:131
286. Oppenheimer BR, Kulkarni SR, Nakajima T, Matthews K. 1995. *Science* 270:1478
287. Padoan P, Nordlund Å. 2002. *Astrophys. J.* 576:870
288. Padoan P, Nordlund Å. 2004. *Astrophys. J.* 617:559
289. Palla F, Baraffe I. 2005. *Astron. & Astrophys.* 432:L57
290. Palla F, Stahler SW. 2002. *Astrophys. J.* 581:1194
291. Parker RJ, et al. 2011. *MNRAS* 412:2489
292. Pascucci I, et al. 2009. *Astrophys. J.* 696:143
293. Patience J, King RR, De Rosa RJ, Marois C. 2010. *Astron. & Astrophys.* 517:A76
294. Pecaut MJ, Mamajek EE, Bubar EJ. 2012. *Astrophys. J.* in press
295. Peña Ramírez K, et al. 2011. *Astron. & Astrophys.* 532:A42
296. Phan-Bao N, et al. 2008. *Astrophys. J.* 689:L141
297. Phan-Bao N, et al. 2011. *Astrophys. J.* 735:14
298. Pinfield DJ, et al. 2008. *MNRAS* 390:304
299. Rathborne JM, et al. 2009. *Astrophys. J.* 699:742
300. Rayner JT, et al. 2003. *Pub. Astron. Soc. Pacific* 115:362
301. Rebolo R, Zapatero Osorio MR, Martín EL. 1995. *Nature* 377:129

302. Rebolo R, et al. 1996. *Astrophys. J.* 469:L53
303. Rebull LM, et al. 2006. *Astrophys. J.* 646:297
304. Rebull LM, et al. 2010. *Astrophys. J. Suppl.* 186:259
305. Rees MJ. 1976. *MNRAS* 176:483
306. Reid IN, Gizis JE, Hawley SL. 2002 *Astron. J.* 124:2721
307. Reid IN, et al. 1999. *Astrophys. J.* 521:613
308. Reipurth B, Clarke C. 2001. *Astron. J.* 122:432
309. Reiners A. 2009. *Astrophys. J.* 702:L119
310. Reiners A, Basri G. 2008. *Astrophys. J.* 684:1390
311. Reiners A, Basri G. 2010. *Astrophys. J.* 710:924
312. Reiners A, et al. 2007. *Astrophys. J.* 671:L149
313. Reylé C, et al. 2010. *Astron. & Astrophys.* 522:A112
314. Riaz B, Gizis JE. 2008. *Astrophys. J.* 681:1584
315. Riaz B, Gizis JE, Harvin J. 2006. *Astron. J.* 132:866
316. Rice EL, Faherty JK, Cruz KL. 2010. *Astrophys. J.* 715:L165
317. Rice EL, et al. 2010. *Astrophys. J. Suppl.* 186:63
318. Rice WKM, et al. 2003. *MNRAS* 346:L36
319. Rieke GH, Rieke MJ. 1990. *Astrophys. J.* 362:L21
320. Rodríguez DR, Bessell MS, Zuckerman B, Kastner JH. 2010. *Astrophys. J.* 727:62
321. Rodríguez-Ledesma MV, Mundt R, Eisloffel J. 2009. *Astron. & Astrophys.* 502:883
322. Scelsi L, et al. 2007. *Astron. & Astrophys.* 468:405
323. Schlieder JE, Lépine S, Simon M. 2010. *Astron. J.* 140:119
324. Schmidt SJ, West AA, Hawley SL, Pineda JS. 2010. *Astron. J.* 139:1808
325. Scholz A, Eisloffel J. 2004. *Astron. & Astrophys.* 421:259
326. Scholz A, Eisloffel J. 2005. *Astron. & Astrophys.* 429:1007
327. Scholz A, Jayawardhana R. 2006. *Astrophys. J.* 638:1056
328. Scholz A, Jayawardhana R, Wood K. 2006. *Astrophys. J.* 645:1498
329. Scholz A, et al. 2007. *Astrophys. J.* 660:1517
330. Scholz A, et al. 2008. *Astrophys. J.* 681:L29
331. Scholz A, et al. 2011. *MNRAS* 413:2595
332. Scholz R-D, McCaughrean MJ, Zinnecker H, Lodieu N. 2005. *Astron. & Astrophys.* 430:L49
333. Seifahrt A, Reinders A, Almaghrbi KAM, Basri G. 2010. *Astron. & Astrophys.* 512:A37
334. Shen S, Wadsley J, Hayfield T, Ellens N. 2010. *MNRAS* 401:727
335. Shkolnik E, Liu MC, Reid IN. 2009. *Astrophys. J.* 699:649
336. Shkolnik E, et al. 2011. *Astrophys. J.* 727:6
337. Silk J. 1977. *Astrophys. J.* 214:152

338. Sills A, Pinsonneault MH, Terndrup DM. 2000. *Astrophys. J.* 534:335
339. Simon M, Dutrey A, Guilloteau S. 2000. *Astrophys. J.* 545:1034
340. Skemer AJ, et al. 2011. *Astrophys. J.* 732:107
341. Skrutskie MF, et al. 2006. *Astron. J.* 131:1163
342. Slesnick CL, Carpenter JM, Hillenbrand LA. 2006. *Astron. J.* 131:3016
343. Slesnick CL, Hillenbrand LA, Carpenter JM. 2004. *Astrophys. J.* 610:1045
344. Slesnick CL, Hillenbrand LA, Carpenter JM. 2008. *Astrophys. J.* 688:377
345. Smith RJ, Clark PC, Bonnell IA. 2009. *MNRAS* 396:830
346. Song I, Zuckerman B, Bessell MS. 2004. *Astrophys. J.* 600:1016
347. Spiegel DS, Burrows A, Milsom JA. 2011. *Astrophys. J.* 727:57
348. Stamatellos D, Hubber DA, Whitworth AP. 2007. *MNRAS* 382:L30
349. Stamatellos D, Whitworth AP. 2009. *MNRAS* 392:413
350. Stamatellos D, Whitworth A, Maury A, André P. 2011. *MNRAS* 413:1787
351. Stassun KG, Mathieu RD, Mazeh T, Vrba FJ. 1999. *Astron. J.* 117:2941
352. Stassun KG, Mathieu RD, Valenti, JA. 2006. *Nature* 440:311
353. Stassun KG, Mathieu RD, Valenti, JA. 2007. *Astrophys. J.* 664:1154
354. Stauffer JR, Hamilton D, Probst RG. 1994. *Astron. J.* 108:155
355. Stauffer JR, Hartmann L. 1986. *Pub. Astron. Soc. Pacific* 98:1233
356. Stauffer JR, Schultz G, Kirkpatrick JD. 1998. *Astrophys. J.* 499:L199
357. Stauffer JR, et al. 1989. *Astrophys. J.* 344:L21
358. Stauffer JR, et al. 2007. *Astrophys. J. Suppl.* 172:663
359. Steele IA, Jameson RF. 1995. *MNRAS* 272:630
360. Stelzer B, Micela G, Neuhäuser R. 2004. *Astron. & Astrophys.* 423:1029
361. Sterzik MF, et al. 2004. *Astron. & Astrophys.* 427:245
362. Terndrup DM, et al. 2000. *Astron. J.* 119:1303
363. Thies I, et al. 2010. *Astrophys. J.* 717:577
364. Todorov K, Luhman KL, McLeod, KK. 2010. *Astrophys. J.* 714:L84
365. Umbreit S, et al. 2005. *Astrophys. J.* 623:940
366. Vorobyov EI, Basu S. 2009. *Astrophys. J.* 703:922
367. Weights DJ, et al. 2009. *MNRAS* 392:817
368. Werner MW, et al. 2004. *Astrophys. J. Suppl.* 154:1
369. Whelan ET, et al. 2005. *Nature* 435:652
370. Whelan ET, et al. 2009. *Astrophys. J.* 706:1054
371. White RJ, Basri G. 2003. *Astrophys. J.* 582:1109
372. White RJ, Ghez AM. 2001. *Astrophys. J.* 556:265
373. White RJ, Ghez AM, Reid IN, Schultz G. 1999. *Astrophys. J.* 520:811
374. White RJ, Hillenbrand LA. 2004. *Astrophys. J.* 616:998
375. Whitworth AP, Stamatellos D. 2006. *Astron. & Astrophys.* 458:817

- 376. Whitworth AP, Zinnecker H. 2004. *Astron. & Astrophys.* 427:299
- 377. Whitworth A, et al. 2007. In *Protostars and Planets V.* ed. B Reipurth, D Jewitt, K Keil, Tucson:University of Arizona Press 459
- 378. Wright EL, et al. 2010. *Astron. J.* 140:1868
- 379. York DG, et al. 2000. *Astron. J.* 120:1579
- 380. Young CH, et al. 2004. *Astrophys. J. Suppl.* 154:396
- 381. Zapatero Osorio MR, Rebolo R, Martín EL. 1997. *Astron. & Astrophys.* 317:164
- 382. Zapatero Osorio MR, et al. 2000. *Science* 290:103
- 383. Zapatero Osorio MR, et al. 2002. *Astrophys. J.* 578:536
- 384. Zapatero Osorio MR, et al. 2006. *Astrophys. J.* 647:1405
- 385. Zapatero Osorio MR, et al. 2007. *Astrophys. J.* 666:1205
- 386. Zapatero Osorio MR, et al. 2008. *Astron. & Astrophys.* 477:895
- 387. Zapatero Osorio MR, et al. 2010. *Astrophys. J.* 715:1408
- 388. Zapatero Osorio MR, et al. 2011. *Astrophys. J.* 740:4
- 389. Zuckerman B, Rhee JH, Song I, Bessell MS. 2011. *Astrophys. J.* 732:61
- 390. Zuckerman B, Song I. 2004. *Ann. Rev. Astron. Astrophys.* 42:685

6 Sidebar

6.1 The Discovery of Brown Dwarfs

The following should appear near the introduction:

The existence of brown dwarfs was predicted in the 1960's (Hayashi & Nakano 1963, Kumar 1963), but they were not found until more than two decades later. One of the first promising candidates was GD 165 B, which was discovered as a companion to a white dwarf (Becklin & Zuckerman 1988). This object was the first known member of the L spectral class of cool dwarfs ($T_{\text{eff}} = 1500\text{--}2500$ K, Kirkpatrick, Henry & Liebert 1993) and could be either a very low-mass star or a brown dwarf (Kirkpatrick et al. 1999b). Through radial velocity measurements of the star HD 114762, Latham et al. (1989) detected the presence of a close, unseen companion with a minimum mass of $11 M_{\text{Jup}}$. It is likely a massive planet or a brown dwarf, although its substellar nature is not guaranteed since the inclination of its orbit is unknown. The first unambiguous example of a brown dwarf was the companion Gl229 B (Nakajima et al. 1995), which exhibited strong methane absorption that firmly established that it was too cool to be a star (Oppenheimer et al. 1995). Near the time that Gl229 B was discovered, PPl 15 and Teide 1 were identified as promising brown dwarf candidates in the Pleiades open cluster (Rebolo, Zapatero Osorio & Martín 1995; Stauffer, Hamilton & Probst 1994). They were confirmed as substellar by the detection of Li absorption (Basri, Marcy & Graham 1996; Rebolo et al. 1996), making them the first known free-floating brown dwarfs.

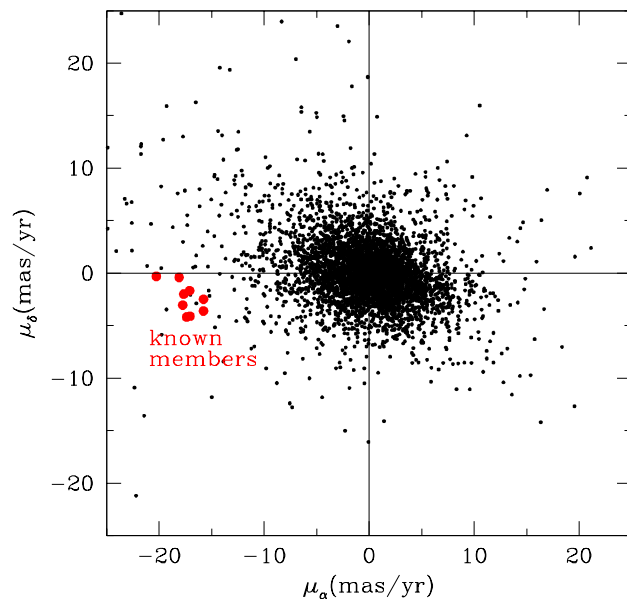


Figure 1: Proper motions of stars in Chamaeleon I measured from two epochs of *HST*/ACS images (J. Bochanski, in preparation). The motions of the known members within these images are indicated (*large red points*).

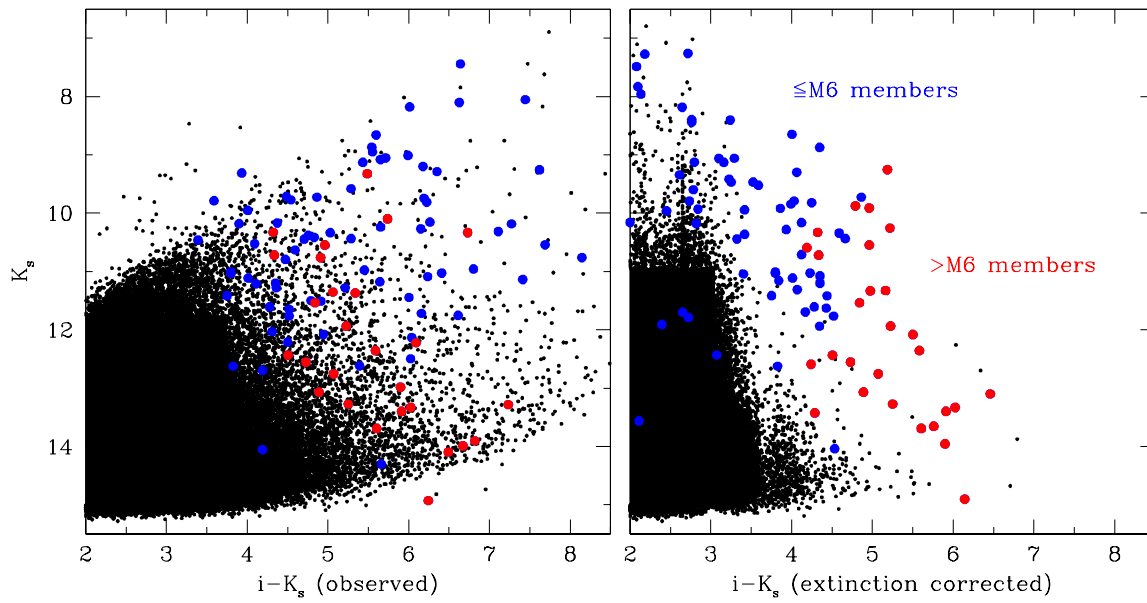


Figure 2: Observed and extinction-corrected color-magnitude diagrams for the portion of Taurus imaged by SDSS (Finkbeiner et al. 2004). The known members of Taurus are indicated (*large blue and red points*). The i and K_s data are from SDSS and 2MASS, respectively.

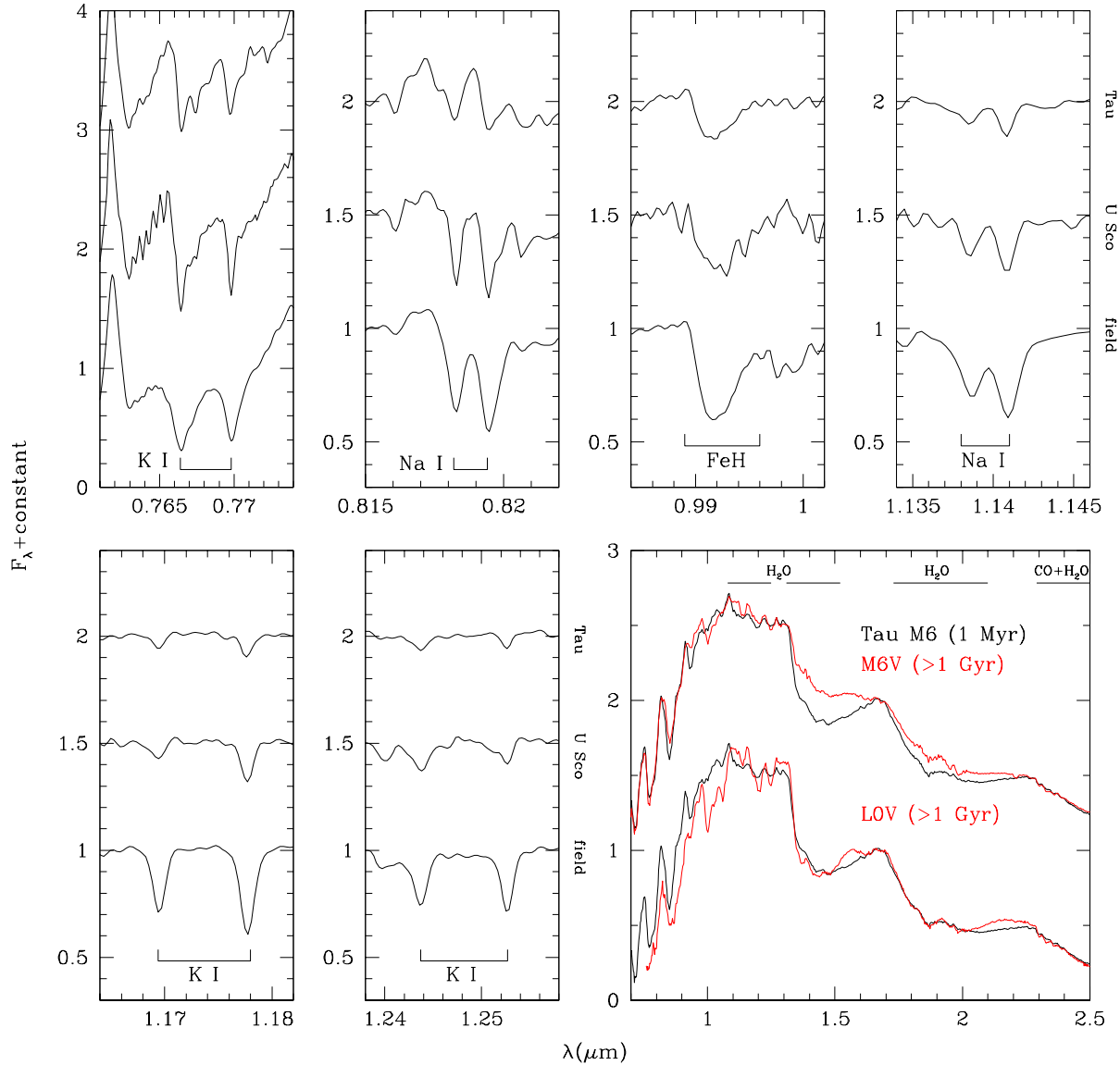


Figure 3: The top and left panels show gravity-sensitive absorption lines for late-M members of Taurus ($\tau \sim 1$ Myr), Upper Sco ($\tau \sim 12$ Myr), and the field ($\tau \gtrsim 1$ Gyr, Luhman et al. 2007b). In the lower right panel, a low-resolution spectrum of an M6 member of Taurus is compared to data for M6V and L0V field dwarfs, illustrating how the strength of H₂O absorption and the shape of the H- and K-band continua depend on gravity.

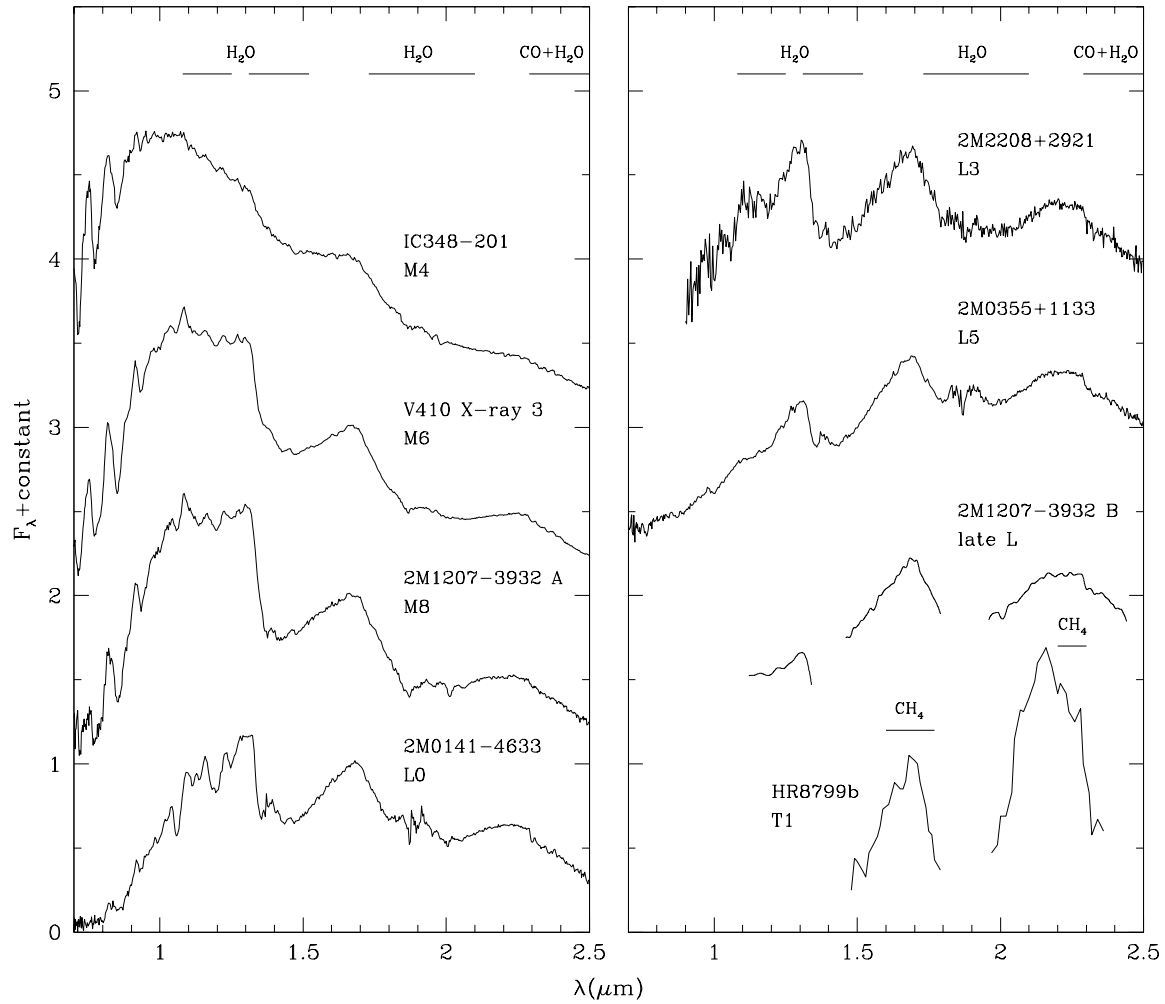


Figure 4: Low-resolution spectra of young objects ($\tau \sim 1\text{--}50$ Myr) from mid-M to early T (Barman et al. 2011a, Kirkpatrick et al. 2006, Morrow et al. 2008, Muench et al. 2007, Patience et al. 2010). The data are normalized at $1.68 \mu\text{m}$.

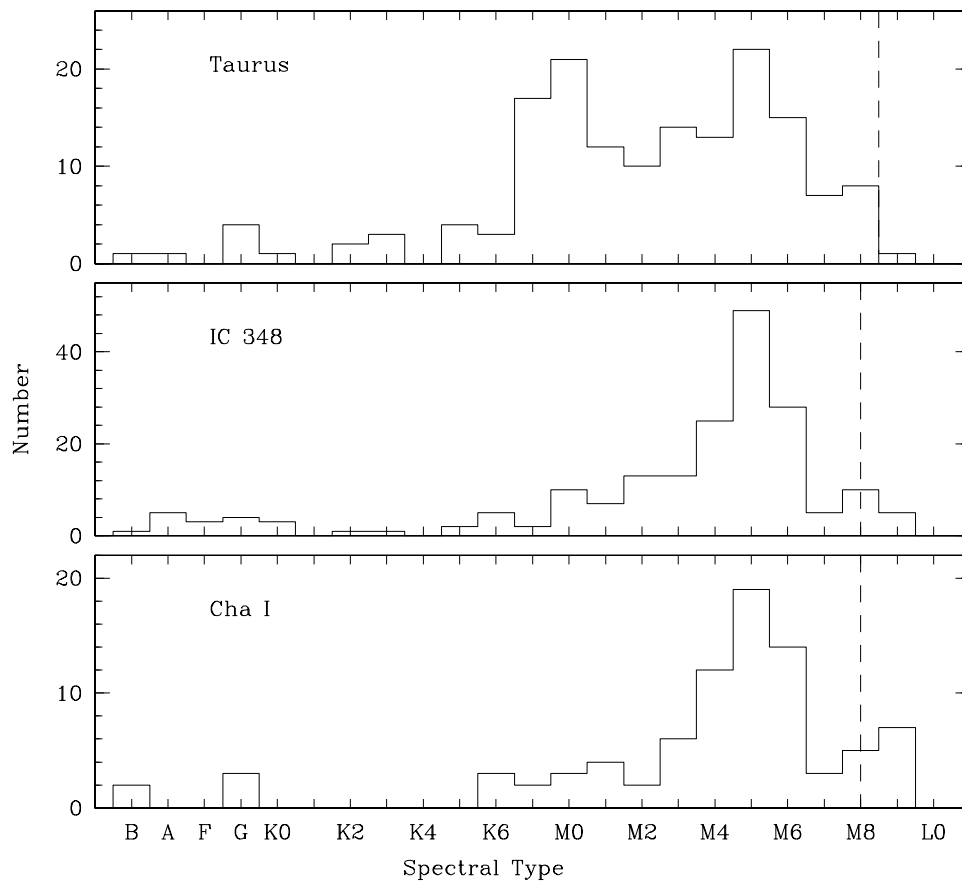


Figure 5: Distributions of spectral types for representative samples of members of Taurus ($\tau \sim 1$ Myr), IC 348 ($\tau \sim 2-3$ Myr), and Chamaeleon I ($\tau \sim 2-3$ Myr, Luhman 2007, Luhman et al. 2009b, 2003b). The completeness limits of these samples are indicated (*dashed lines*).

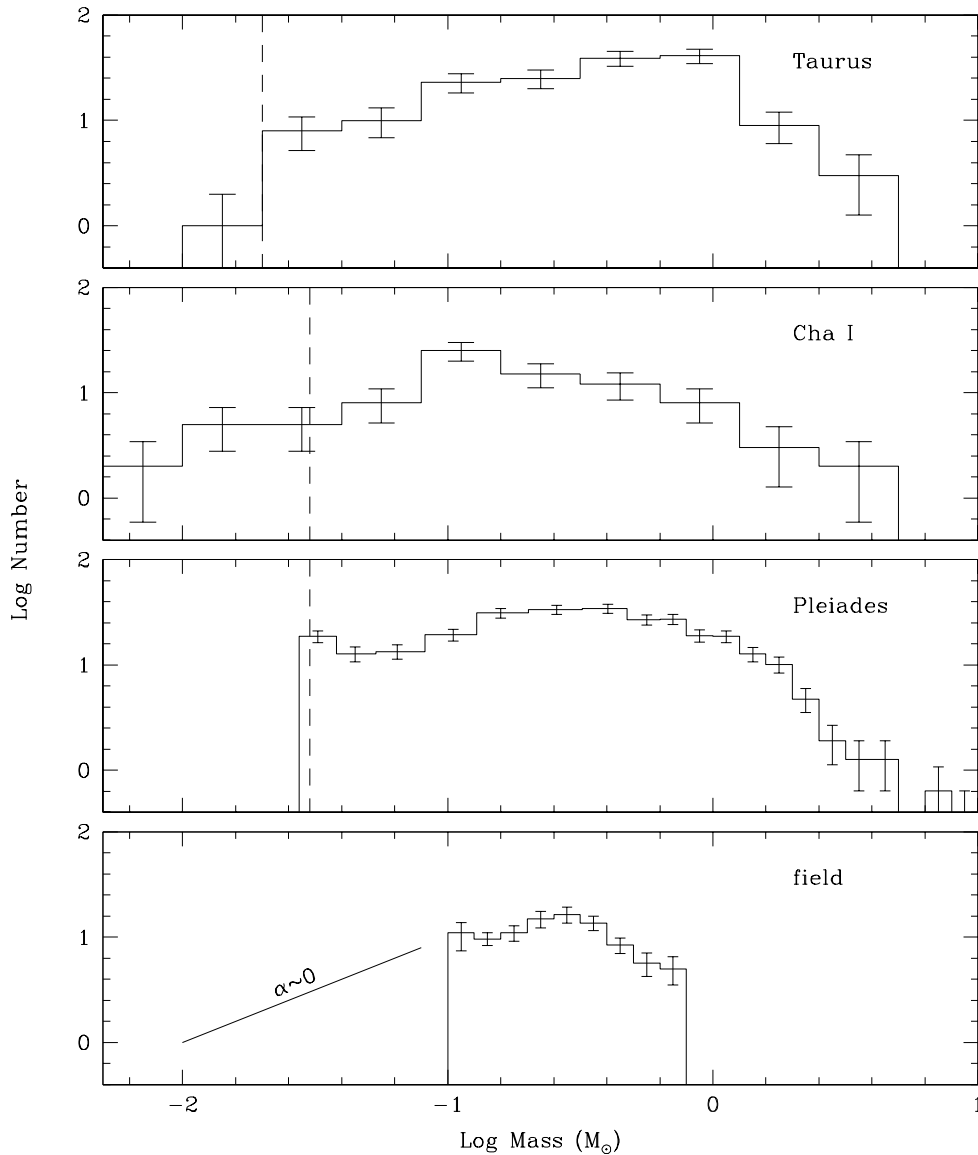


Figure 6: IMFs for Taurus, Chamaeleon I, the Pleiades, and the field (Bochanski et al. 2010; Luhman 2007; Luhman et al. 2009b; Moraux, Kroupa & Bouvier 2004). Assuming a power-law form for the mass function of brown dwarfs, surveys of the field indicate a slope of $\alpha \sim 0$ in linear units, or $\Gamma = -1$ in the logarithmic units plotted in this diagram (Burningham et al. 2010, Kirkpatrick et al. 2011, Metchev et al. 2008, Reyl   et al. 2010). The data for the Pleiades and the field have been scaled to fit within the same limits used for Taurus and Chamaeleon I. The completeness limits of the cluster samples are indicated (*dashed lines*).

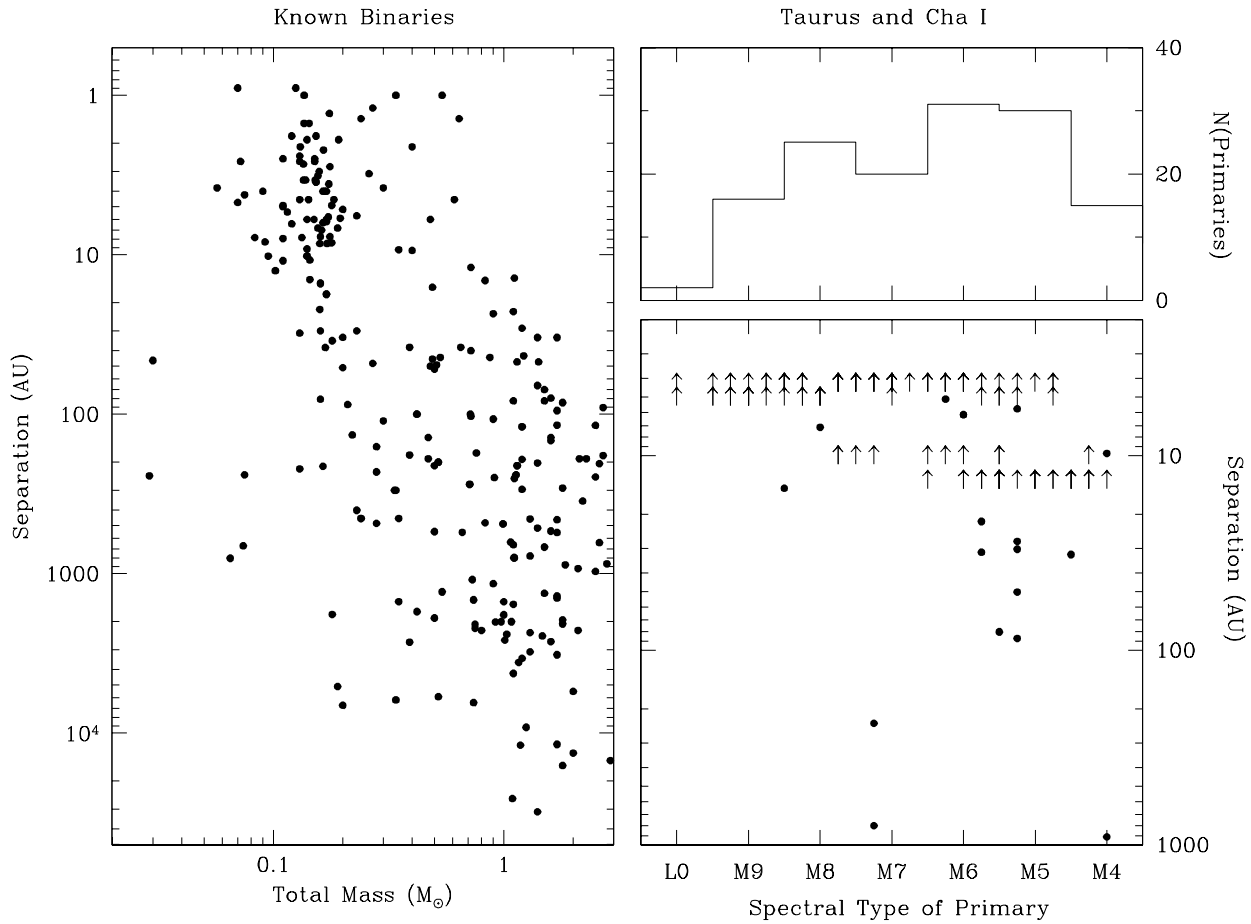


Figure 7: *Left*: Projected separation versus total system mass for a compilation of known binaries (Faherty et al. 2011). *Right*: Projected separation of resolved binaries (*points*) and the detection limits for unresolved sources (*arrows*) versus primary spectral type in Taurus and Chamaeleon I (Konopacky et al. 2007; Kraus, White & Hillenbrand 2006; Lafrenière et al. 2008; Neuhäuser et al. 2002, K. Todorov, in preparation). The number of primaries as a function of spectral type is shown with the histogram.

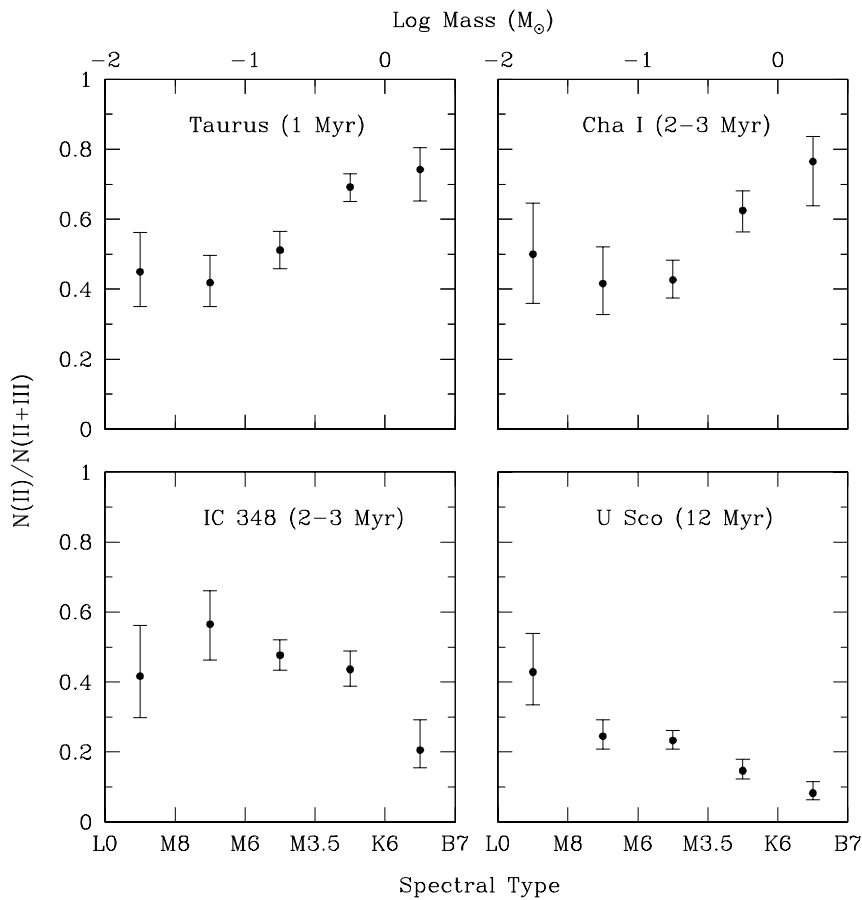


Figure 8: Fraction of sources with primordial circumstellar disks (class II) as a function of spectral type in Taurus, Chamaeleon I, IC 348, and Upper Sco (Lada et al. 2006, Luhman et al. 2005a, 2008, 2010, Muench et al. 2007, K. Luhman, in preparation). Stars with debris disks are designated as class III. The boundaries of the spectral type bins have been chosen to correspond approximately to logarithmic intervals of mass.

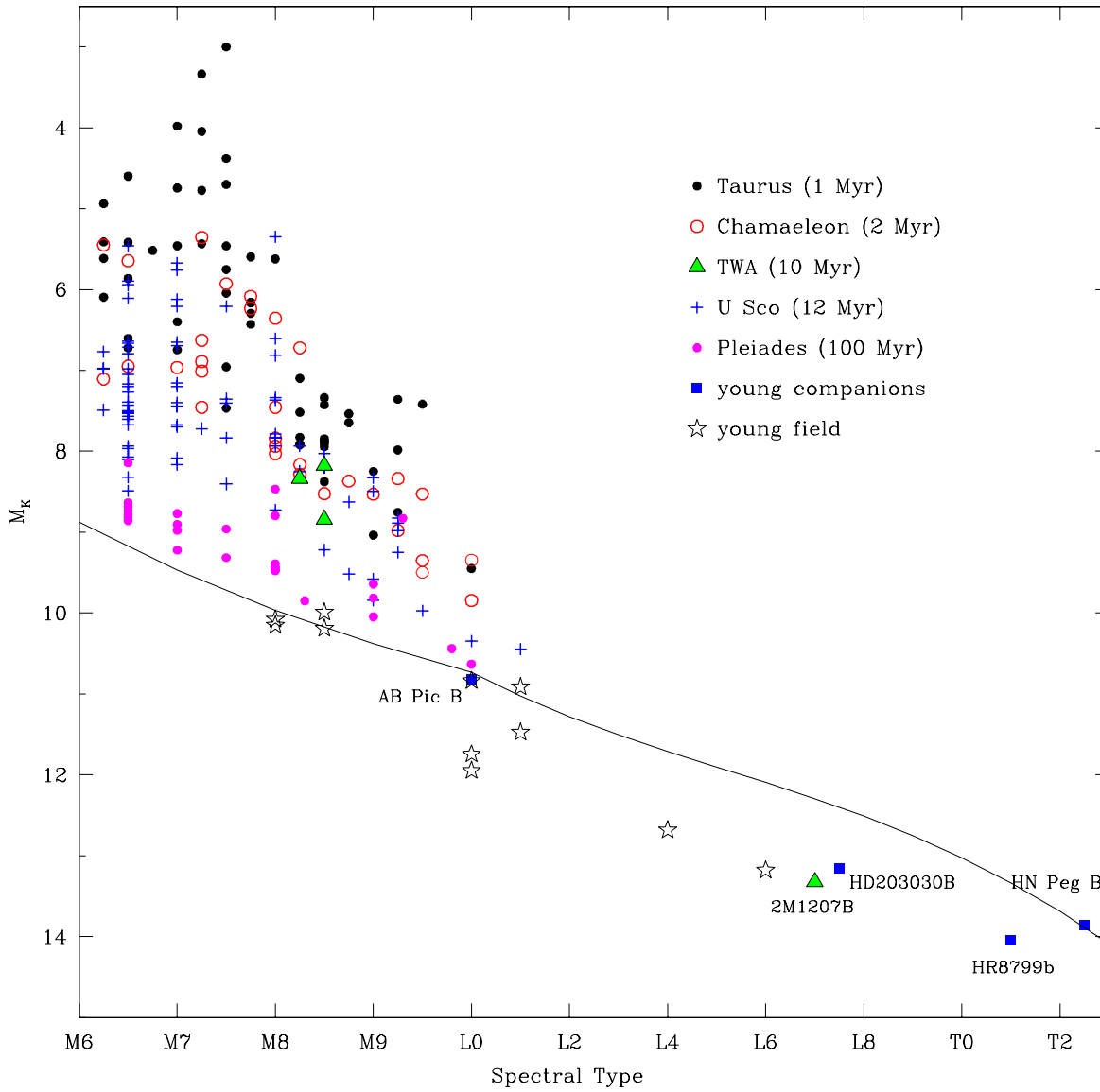


Figure 9: M_K versus spectral type for young late-type objects in nearby associations, clusters, multiple systems, and the field. A fit to data for normal, older field dwarfs is shown (*solid line*, Faherty et al. 2012).